A Security-Constrained Hydrothermal Unit Commitment Model in the Day-Ahead Electricity Market

Preprint PISIS-RR22-01
Graduate Program in Systems Engineering, UANL
San Nicolás de los Garza, NL, Mexico

Uriel I. Lezama-Lope
Universidad Autónoma de Nuevo León (UANL)
Graduate Program in Systems Engineering
uriel.lezama@ineel.mx

Roger Z. Ríos-Mercado
Universidad Autónoma de Nuevo León (UANL)
Graduate Program in Systems Engineering
roger.rios@uanl.edu.mx

José Luis Ceciliano-Meza
Tecnológico de Monterrey
Department of Industrial Engineering
joseluis.ceciliano@tec.mx

June 2022

Abstract

In 2015, the Ministry of Energy created a wholesale electricity market in Mexico. As a result, the country shifted from a vertically integrated regulation to a competitive market framework. In this context, the day-ahead market is essential to plan better the generation and sales of energy. This paper evaluates a hydro-thermal security-constrained unit commitment model and its solution method. The objective function determines the maximum economic surplus of the participants in the market. The problem is modeled as a mixed-integer non-linear programming incorporating real-world constraints from the particular problem and a hydropower generator function non-linear features.

A decomposition approach that solves a master problem and a series of subproblems is developed. Furthermore, a new component has been added to deal with the non-linear features of the hydropower generator function using a first-order Taylor's approximation. Simulation results are presented starting by solving a representative case of the electricity market in Mexico, demonstrating its use. Moreover, to evaluate the performance, multiple instances are created from publicly available information on the day-ahead market in Mexico. The model can be helpful in markets with sizable hydropower sources to obtain a more accurate and timely system operation scheduling.

Keywords: Electricity market; unit commitment; mixed-integer linear programming; short-term hydro scheduling; hydro power production function; ancillary services.

1 Introduction

Electricity fuels our modern life; it kindles our homes, powers our factories, lights up our classrooms, supplies our hospitals, illuminates our streets, and throws light upon many other activities. The demand depends on human behavior and it varies during the day. Since storing electricity in considerable quantities is unfeasible yet, electric generators must produce only the amount of energy required for consumption. Therefore, we have to schedule just the amount of generating power for each hour. Also, this scheduling must be done safely and reliably for the electrical system. The Unit Commitment Problem (UCP) is a decision-making problem that determines which generators must be turned on and off at each time period, and establishes how much power these generators must produce to meet loads at a minimal cost. Naturally, depending on particular problem specifics, many variations of the UCP have been studied in the literature. A survey of the evolution of UCP models and solution methods can be found in Abdou and Tkiouat [1] and Saravanan et al. [33].

The basic UCP has a set of generators (with different production costs) and loads connected to an electric network. Along these features, many constraints must be met: the most important ones related to the security system is load balancing, which allows to keep the frequency system within safety levels. Other constraints are related to the technical features of generators such as power limits, ramps, minimum up-time, and minimum down-time. Another important requirement related to network operation is to keep the transmission power flow within safe limits.

UCP models are widely used in several countries for planning power production. Each country extends the basic UCP model with its particular features depending on its energy policies. The resulting mathematical model encompasses different constraints and objective functions. The UCP models were originally proposed and applied in monopolistic contexts and have been extended to generate production schedules for a competitive market environment. For instance, the UCP models are used in countries with a competitive market environment to schedule the production based on sales and purchase bids. In this case, models seek to maximizes profits for the participants in the market.

In this paper, we address a UCP for the day-ahead market (DAM) in Mexico that uses the sales offers and purchase bids of the participants (generators and loads) in the market. Besides, it incorporates other constraints such as the transmission losses, power flow limits in tie-lines, five simultaneous reserves with different timing, technical features of hydraulic generators such as the Hydropower Generator Function (HPF), balanced in the hydraulic network (levels and flows in reservoirs and rivers). Moreover, the objective function determines the maximum economic surplus of the participants.

A mixed-integer non-linear programming model is proposed for solving this problem where the binary integer variables indicate the decisions of turning on and off generators and supply or not a specific type of reserve. The continuous variables represent the decision of the amount of energy and reserve they must produce. Some simplifications are made to reduce it into a mixed-integer linear program (MILP).

A cut generation strategy embedded into a decomposition method is developed for solving this model; this strategy entails decomposing the problem into a master problem (MP) and a series of non-linear sub-problems (SP). On the one hand, the MP is an MILP that solves the generators' schedule indicating which should be turned on or off. On the other hand, the SP calculate the power flow and transmission losses solving a DC power flow method. The main goal of the sub-problems is to find out the power flow in the tie-lines and calculate the power losses in the network. In addition, a feasibility test identifies the transmission limits that are violated. Then, the transmission constraint violations are added to the master problem. The method ends when no more violations in the transmission network are found, and a tolerance is reached. An innovative feature of this model is the handling of the non-linear HPF that calculates the generation hydraulic depending on the height head water reservoir and the water flux in the turbine using the first-order Taylor polynomial approximation. Moreover, the approximation is performed at each iteration of the algorithm.

Several tests to demonstrate that the model is consistent and applicable to markets requiring hydrothermal coordination were carried out. First, a case study with the electricity system of Mexico is presented, with results demonstrating a consistent behavior between energy prices and demand, a suitable estimate of losses, and a satisfactory hydraulic balance. Second, performance tests were carried out with 320 instances built from public information from the Independent System Operator (ISO) in Mexico. The objective is to measure mainly solution times, transmission lines' power flow violations, and the loss approximation error. In all instances, the tolerance required is achieved.

The remaining sections of this paper are organized as follows: Section 2 briefly presents the main characteristics of the Wholesale Electricity Market in Mexico. Section 3 showcases a survey of the main works in UCP models focused on electricity markets and hydro-thermal coordination. Section 4 shows the mathematical model of the DAM studied in this paper. Section 5 details the solution method proposed in this work. The application of the proposed methodology is put forward in Section 6. Finally, in section 7 the conclusions and possible extensions are discussed.

2 Wholesale electricity market in Mexico

The electricity sector in Mexico was vertically integrated, where the generation, planning and operation of the system were controlled by the state. The federal government operated, generated, transmitted, distributed and commercialized electric power. In this context, the UC problem was used to minimize the generators production costs [7]. The participation of the private companies in the energy sector was limited.

In 2015, the Ministry of Energy created the wholesale electrical market in Mexico (WEM). With this, Mexico shifted from a vertically integrated regulation to a competitive market framework. The rules of new framework were published in [25]. Furthermore, an ISO was created which has legal authority over the electrical network and manages the WEM. The main activities of ISO are: receiving participants' offers and bids, planning and operating the electrical system, protecting its security and reliability, dispatching instructions to generators, paying for the electricity charges and cashing in participants. The participants in the marker will be categorized as energy buyers and sellers. They make a offers and bids. A offer is a financial proposal of a participant (seller) that represents the cost of a market traded product. The offer is a series of paired data that represents the relationship of the power offer in MW and its cost in $/MWh; the series of paired data forms a straight-line segments function with incremental monotonically features. Similarly, bid is a financial proposal of a participant (buyer) that represents how much is it willing to pay for the market traded products. The bid is a series of paired data that represents the relationship of the power required in MW and its price in $/MWh; the series of paired data forms a straight-line segments function with diminishing monotonically features.

The products traded in the DAM are:

- Energy: power produced by each power station.
- Ancillary services: products related to the safely and reliably operation of the electric system like power reserves.

From all ancillary services like regulation, reserves, emergency start-up, island mode operation and dead bus connection, only regulation and reserve are supplied competitively through market mechanisms.

2.1 Day-ahead market in Mexico

DAM is applied by calculating the unit status and power generation for every hour, for the next 24 hours of the next day. The DAM model optimizes both energy and the different types of reserves. The main inputs are sale offers of the generators, the purchase bid of the elastic demands and fixed load demand, which will be entered into the optimization model. The rules of the DAM processes are described in [27] and [26]. An important step is to calculate the marginal prices per node, with this value the energy produced is paid to participants. Next, the main features of the reserve traded in the market are described follows.

The reserves offers are committed to the generators based on theirs offers and the requirements established by ISO. Moreover, the different types of reserves are time-dependent and offered by generators are classified as follows:

- **Regulation reserve (RRe)** can be provided by the generators equipped to connect to automatic generation control (AGC) that is administrated by ISO. The AGC is a control system that increases or lowers the power of generators in real-time to keep the system's frequency within safe limits by keeping the balance between loads and generation automatically.
- **The spinning reserve (RRo)** is the unused capacity of generators connected to the network to supply power in a given time (10 and 30 minutes).
- **The non-spinning reserve (RNRo)** is the unused capacity of generators not connected to the network to supply power in a given time (10 and 30 minutes).

The ISO established the reserve requirements that are introduced as restrictions in the optimization model. These requirements have a market value, given by a Operating Reserve Demand Curve (ORDC), which represents how much ISO is willing to pay for each reserve in line with the levels of security and reliability required. [31] has developed a method to calculate the ORDC in Mexico. Moreover, the requirement of different types of reserves are calculated by ISO. The requirements are classified as follows:

- **The regulation reserve (RRE)** is met by the sum of unused capacity of generators connected to the network and controlled by AGC system.
- **The spinning reserve (RRR)** is met by the sum of unused capacity of generators connected to the network to supply power within the next 10 minutes, plus the total of regulation reserve committed.
- **The operative reserve (RRO)** is met by the sum of unused capacity of generators connected and not connected (capable of starting-up) to the network to supply power within the next 10 minutes, plus the total of regulation reserve committed.
- **The supplementary reserve (RRS)** is met by the sum of unused capacity of generators connected and not connected (capable of starting-up) to the network to supply power within the next 10 and 30 minutes, plus the total of the operative reserve and the total regulation reserve committed.

3 Related work

The literature on unit commitment (UC) models is vast. UCP problems can be classified according to three sets of constraints: generators operating constraints, electrical network constraints and system constraints. The first set includes generation limits, ramps, minimum up and downtimes, fixed or variables start-up costs, etc. The second group comprises limits in lines and tie-lines. The last one encompasses meeting demand and load-generation balance. Anjos and Conejo [2] outline some examples of these models. However, most recent research on basic UCP deals with finding tight and compact (T&C) formulations [30, 29, 20, 37]. These T&C models have shown promising results because they can be extended with additional constraints.

For a UCP model to work properly in a real-world environment, it is necessary to add operational constraints of the electrical system in the country. For example, the inclusion of the electrical network is essential in a real model focusing on security; the calculation of losses are important to include in the system operation costs, and load-generation balance; the modeling of combined cycle plants is necessary for the right operation of the units comprising the plant; the coordination between hydraulic and thermal generation sources impact in the future costs and secure operation system as well as the security in reservoirs and rivers; the limitations of fuel and water are paramount for doing a realistic schedule. Finally, it is necessary to take into account intermittent energy produced by the renewable energy generators.

With the rise of competitive electric markets, UCP models have changed from minimizing production costs to maximizing profits or maximizing social welfare; the new markets model includes the previous UCP constraints but adds new variants to meet new economic regulations. An investigation that shows the role of UCP models in the market environment can be found in Hobbs et al. [19].

Some market UCP models used in this work are mentioned below. In Bisanovic et al. [5], a market UCP model is presented in high detail, although the paper focuses on handling long-term bilateral contracts and considers operating constraints generators and was tested on a small electrical system. It is worth noting that this work uses a model with three sets of binary variables introduce by Garver [15] to reduce the computational burden. Chow et al. [8] present the model of optimization between energy and ancillary service in New York ISO. This model includes different types of reserve, for example, spinning or non-spinning, of 10-min or 30-min depending on the power that can be achieved in a given time. Ma et al. [22] present the security-constrained unit commitment and dispatch model that is implemented for Midwest ISO's DAM, it optimizes both energy and ancillary services. The model integrates operational generation constraints, such as power min/max limits, regulation min/max limits, ramp-rate limits, min/max-run time and min-down time. In this case, the problem is modeled in two parts. The first one represents a security constraint unit commitment using a MIP. The second one represents an economic dispatch using a LP. In the first instance, a commercial solver resolves the MIP and sends the status of the generators to the model LP including transmission constraints. Then a commercial solver resolves the LP. In the end, a feasibility test is carried out. the model is solved using a MIP and LP for the UCP adding iterative violated transmission constraints. In these previous market models, the hydrothermal coordination is not included.

Solving a hydrothermal coordination is important for effective planning of the operation electrical system which consists of finding the optimal commitment and dispatch of thermal and hydro generation resources for every hour. In the following section, some works related to hydrothermal coordination modeling are presented. Babona and Rossell Pujós [3] introduce an uncoupled formulation of the whole hydrothermal coordination and solves it with a MIP commercial solver (CPLEX); the model includes a linear power hydro generation constraint that is dependent on the height head and the volume water of the reservoir, and it also encompasses spinning reserve, network constraints (balance), and minimum up and downtimes of thermal units. Although these are basic constraints, the model lacks other important operational constraints for effective real-life operation.

Unlike the previous model, Yu et al. [38] include several operational and hydro constraints such as power balance, power losses, hydro production, generation limits, unit reserves, system spinning reserves requirements, minimum up and downtime of the units, water storage balance, water storage limits, water discharge limits, the relationship between water head and water storage, and import/export limits. The model solves the MIP-based hydrothermal coordination using commercial optimization solvers such as CPLEX, OSL, and ZOOM. Conejo et al. [9] set forth a MIP-based formulation including the relationship between hydropower production, water discharge, and water head. The major contribution of this model is to formulate a self-scheduling of a hydro-generating company participating in the day-ahead power pool electricity market with the hydro component. The authors employ a family of discretized curves per unit to account for the nonlinear relationship between the reservoir head, the power output of the hydro unit, and the water discharged. In this model, a particular curve is used depending on reservoirs volume. Even though the model includes cascaded reservoirs, the authors overlook the time that water takes to get from an upstream reservoir to a downstream reservoir (water travel time delays) by considering one-hour delays. Finally, the model also lacks a thermal unit commitment. An study that integrates travel time delays of water, though not explicitly, can be found in Gil et al. [17].

Catalão et al. [6] put forward a model that fixes those flaws and outline a mixed-integer quadratic programming model for scheduling of pure cascaded hydro systems. The thermal system does not consider water travel time delays. Some advantages of the model are incorporating head dependency, operating restricted zones and discharge ramping constraints; and integrating the effect of the changes in the head in a single function of water discharge and water storage instead of deriving several curves for different heads. The authors explain that the discretization of the nonlinear dependence between power generation, water discharge, and head, by deriving several curves for different heads as depicted in Conejo et al. [9], which increases the computational load required to solve the scheduling of hydro generation. The test models in Catalão et al. [6] are just a few examples with three and seven cascaded reservoirs.

An interesting investigation by Bisanovic et al. [4] lays out a comprehensive model for hydro and thermal generators in a DAM. The model manages a multi-reservoir hydro system with hydraulic coupling between reservoirs, turbine discharge limits, spillage, and reservoir level limits. A piecewise linear function —constructed using the best local efficiency points as breakpoints— models the function of power outputs generators and water discharges. The accuracy of the model depends on the approximation of the piecewise function to the non-linear power-discharge function yet it does not consider the water travel time delays. The authors downgrade the relationship between the water head and volume by using a piecewise linear function. Therefore, they underestimate the hydropower production equation by substituting the water head variable with an average gross water head that is held constant.

A real-world model with a lot of cascaded reservoirs (with 162 hydro plants) can be found in Santos et al. [32] who develops a day-ahead generation schedule in Brazil including limits in reservoir, discharge and spilled outflows, other uses of water, evaporation, water delay times to reservoir, upstream/downstream pumping stations, and re-pumping water to another reservoirs. The hydro generation is modeled by a concave piecewise linear function with coefficients related to storage in the reservoir, turbine and spilled outflows. Although Santos does not elaborate the HPF model, his work adopts a highly detailed model developed by Diniz and Souza [11]. Santos' model includes the thermal generation constraints in high detail as well. The model showcased is all-encompassing and closer to a real-life. To solve the model the authors developed an iterative procedure that uses an interior point method and branch and cut, with CPLEX solver.

In sum, Bisanovic et al. [5], Chow et al. [8], and Ma et al. [22] outline thermal UCP models in some electricity markets in the United States that optimizes energy and reserves similar to the DAM in Mexico. However, those works do not include hydrothermal coordination. Specialized works on hydro generation are Babona and Rossell Pujós [3], Yu et al. [38], and Gil et al. [17], Catalão et al. [6]. They employ different methods to model the relationship between non-linear relationship between the reservoir head, water discharge and generation. Conejo et al. [9] and Bisanovic et al. [4] outline models that includes the hydrothermal coordination component in a DAM. However, their hydraulic modeling can be improved to attain results with more accuracy and less computational work. Santos et al. [32] elaborated a full-fledged model for day-ahead scheduling in Brazil but the calculation of transmission losses is not explicit and different types of ancillary services are omitted. Furthermore, the discontinuous operating zones are not considered either. These aspects are important to obtain an better schedule.

In this paper, to solve the DAM with hydrothermal coordination a MINLP UCP model is solved. The thermal system is modeled in high detail and includes energy and ancillary services offers, power generation limits of units, ramp-up and ramp-down of units, minimum up and downtime for units, variable start-up costs based on Morales-España et al. [28], and start-up times and restricted operating zones based on Daneshi et al. [10]. The hydroelectric system is modeled thoroughly includes discharge limits on units, water balance in reservoirs, limits of water storage, hydro generation dependent on discharge and head, cascaded reservoirs, and water travel time delays. To tackle the non-linearity of the hydro generation is used a first-order Taylor polynomial approximation, which is not the first time that use this method to solve electrical planning field problems. For instance, Šepetanc and Pandžić [34] use it to approximate the non-linearity of the Alternating Current Optimal Power Flow (ACOPF) problem; however, it is the first time, as far as we know, that used to approximate the non-linearity characteristic of hydraulic generation.

Moreover, the model integrates transmission network constraints and losses, and incorporates characteristics of the market in Mexico, such as different types of reserves and minimum generation units in regulation. To solve the model proposed an iterative methods based on the references Viana and Pedroso [36], Tejada-Arango et al. [35] and Marín-Cano et al. [23] is used.

The main contribution of this work consists of introducing an original and highly detailed UCP model that includes the hydraulic network and the hydrothermal coordination in an electricity market. Another contribution is the approximation of the hydro generation non-linear function through a first-order Taylor polynomial approximation embedded into a decomposition approach. To the best of our knowledge, this is the first time that such an approach has been applied to the hydro UCP.

4 Mathematical formulation

4.1 Assumptions

Critical key assumptions to bear in mind:

- The purchase bids and the energy generation in each period represents the average power demand between the beginning and the end of a period.
- The limits of generator output power, reserve capacity and emergency ramp rate may change during the planning horizon.
- The generators that comprised a combined-cycle package are considered a single generator with only one selling offer.
- The selling offers of: energy, reserves, and start-up costs are staircase functions with incremental monotonically features with stairs not necessarily equal. Similarly, the purchase bids of elastic demand are staircase functions with monotonically decreasing features with stairs not necessarily equal.

In the following part the mathematical model used to solve the DAM is explained. Also the parameters and decision variables are defined in Appendix A.

4.2 Objective function

Our goal is to minimize an objective function consists on the costs of start-up generation cost, the minimum generation cost, selling costs of the power supplied by thermal generators, selling costs of the power supplied by hydraulic and renewable generators, costs of reserves supplied by hydraulic and thermal generators minus the profit obtain by the purchase of energy from the elastic demand and purchase of reserve requirements.

$$\begin{aligned}
&\min \sum_{i\in\mathcal{I}} \Bigg\{ \sum_{u\in\mathcal{U}^{\mathrm{TE}}} \Bigg[AR_{u,s} sa_{u,i,s} + \beta_{u,i} mgc_u + \sum_{b\in\mathcal{B}_u^{\mathrm{e.s.o}}} P_{b,u,i}^{e.s.o} gb_{b,u,i} \Bigg] \\
&+ \sum_{u\in\mathcal{U}^{\mathrm{HI}}} P_{u,i}^{o.c} g_{u,i} + \sum_{u\in\mathcal{U}^{\mathrm{RE}}} \sum_{b\in\mathcal{B}_u^{\mathrm{e.s.o}}} P_{b,u,i}^{e.s.o} gb_{b,u,i} - \sum_{d\in\mathcal{D}} \Bigg\{ \sum_{b\in\mathcal{B}_d^{\mathrm{e.p.b}}} P_{b,d,i}^{e.p.b} db_{b,d,i} \Bigg\} \\
&+ \sum_{u\in\mathcal{U}^{\mathrm{TE}}\bigcup\mathcal{U}^{\mathrm{HI}}} \Bigg[P_{u,i}^{10.s.r.o} rro_{u,i}^{10} + P_{u,i}^{10.n.s.r.o} rnr_{u,i}^{10} + P_{u,i}^{30.s.r.o} rro_{u,i}^{30} \\
&+ P_{u,i}^{30.n.s.r.o} rnr_{u,i}^{30} + P_{u,i}^{r.r.o} rre_{u,i} \Bigg] - \sum_{b\in\mathcal{B}^{\mathrm{o.r.d.c}}} P_{b,i}^{o.r.d.c} rco_{b,i} \Bigg\}. \qquad (1)
\end{aligned}$$

The constraints of the problem were divided into six groups: system, generators, hydraulic, network, logical, and additional which are detailed below.

4.3 System constraints

4.3.1 Power balance

The sum of power injections in the nodes n minus the transmission losses must be equal to zero. This is the balance equation outlined as follows:

$$\sum_{n\in\mathcal{N}} iny_{n,i} - Loss_i = 0, \qquad i \in \mathcal{I}. \qquad (2)$$

Where the power injections in a node n in a period i is unpacked as follows:

$$iny_{n,i} = \sum_{u\in\mathcal{U}_n} g_{u,i} - \sum_{d\in\mathcal{D}_n} (DF_{d,i} + \sum_{b\in\mathcal{B}_d^{\mathrm{e.p.b}}} db_{b,d,i}), \qquad n \in \mathcal{N},\ i \in \mathcal{I}. \qquad (3)$$

4.3.2 Loads

The lower and upper limits of the elastic loads are shown as follows:

$$0 \le db_{b,d,i} \le DB_{b,d,i}, \qquad b \in \mathcal{B}_d^{\mathrm{e.p.b}},\ d \in \mathcal{D},\ i \in \mathcal{I}. \qquad (4)$$

4.3.3 Offers reserve and requirements reserve

As stated in Section 2, the WEM is a market that optimizes simultaneously energy and reserves. The reserves are committed to the generators based on theirs offers and the requirements established by the ISO. The different types of reserve offered by generators are classified in:

- Regulation reserve can be provided by the generators equipped to connect to AGC increasing or lowering the power of generators. The associated variable is $(rre_{u,i})$.
- The spinning reserve is the unused capacity of generators connected to the network to supply power in a given time (10 and 30 minutes). The associated variables are $(rro^{10}_{u,i})$ and $(rro^{30}_{u,i})$.
- The non-spinning reserve is the unused capacity of generators not connected to the network to supply power in a given time (10 and 30 minutes). The associated variables are $(rnr^{10}_{u,i})$ and $(rnr^{30}_{u,i})$.

The ISO establishes the reserve requirements $rco_{b,i}$ assigning costs by using a ORDC $(\mathcal{B}^{\text{o.r.d.c}})$. To illustrate better the relationship between offers and requirements the Figure 14 has been designed in terms of the following constraints:

The regulation reserve requirements (RRE) are outlined as follows:

$$\sum_{u \in \mathcal{U}^{\text{TE}} \cup \mathcal{U}^{\text{HI}}} rre_{u,i} \geq \sum_{b \in \mathcal{B}^{\text{r.r.}}} rce_{b,i}, \qquad i \in \mathcal{I}. \tag{5}$$

Spinning reserve requirement (RRR) is met by the sum of unused capacity of generators connected to the network to supply power within the next 10 minutes, plus the total of regulation reserve committed.

$$\sum_{u \in \mathcal{U}^{\text{TE}} \cup \mathcal{U}^{\text{HI}}} (rre_{u,i} + rro^{10}_{u,i}) \geq \sum_{b \in \mathcal{B}^{\text{r.r.}} \cup \mathcal{B}^{\text{10.s.r.}}} rco_{b,i}, \qquad i \in \mathcal{I}. \tag{6}$$

Operative reserve requirement (RRO) is met by the sum of unused capacity of generators connected and not connected (capable of starting-up and producing power) to the network to supply power within the next 10 minutes, plus the total of regulation reserve committed.

$$\sum_{u \in \mathcal{U}^{\text{TE}} \cup \mathcal{U}^{\text{HI}}} (rre_{u,i} + rro^{10}_{u,i} + rnr^{10}_{u,i}) \geq \sum_{b \in \mathcal{B}^{\text{r.r.}} \cup \mathcal{B}^{\text{10.s.r.}} \cup \mathcal{B}^{\text{10.r.}}} rco_{b,i}, \qquad i \in \mathcal{I}. \tag{7}$$

Supplementary reserve requirement (RRS) is met by the sum of unused capacity of generators connected and not connected (capable of starting-up and producing power) to the network to supply power within the next 30 minutes, plus the total of the operative reserve and the total regulation reserve committed.

$$\sum_{u \in \mathcal{U}^{\mathrm{TE}} \cup \mathcal{U}^{\mathrm{HI}}} (rre_{u,i} + rro^{10}_{u,i} + rnr^{10}_{u,i} + rro^{30}_{u,i} + rnr^{30}_{u,i}) \geq \sum_{b \in \mathcal{B}^{\mathrm{o.r.d.c}}} rco_{b,i}, \qquad i \in \mathcal{I}. \tag{8}$$

The reader can find a comprehensive explanation of the relationship between reserve offers and the ISO's requirements in Appendix B.

4.3.4 Limits in reserve requirements

The limits of the regulation and operational reserve requirements are expressed in the following constraints:

$$0 \leq rco_{b,i} \leq ORDC_{b,i}, \qquad b \in \mathcal{B}^{\mathrm{o.r.d.c}},\ i \in \mathcal{I}. \tag{9}$$

4.4 Generator constraints

4.4.1 Generation limits

For thermal generators the power level of an generator amounts to power produced during the start-up process; plus the minimal operative limit of generator; plus the sum of the segment powers associated with each offer segment, the first segment of $\mathcal{B}^{\mathrm{e.s.o}}_u$ includes the production cost from zero to the minimal operative limit.

$$g_{u,i} = gs_{u,i} + \beta_{u,i}\underline{g}_{u,i} + \sum_{b \in \mathcal{B}^{\mathrm{e.s.o}}_u} gb_{b,u,i}, \qquad u \in \mathcal{U}^{\mathrm{TE}},\ i \in \mathcal{I}. \tag{10}$$

For renewable generators, the power level of an generator amounts to the sum of the segment powers associated with each offer segment.

$$g_{u,i} = \sum_{b \in \mathcal{B}^{\mathrm{e.s.o}}_u} gb_{b,u,i}, \qquad u \in \mathcal{U}^{\mathrm{RE}},\ i \in \mathcal{I}. \tag{11}$$

For both, renewable and thermal generators, the power level amounts to the sum of the segments offers is limited.

$$0 \leq gb_{b,u,i} \leq \beta_{u,i} GB_{b,u,i}, \qquad b \in \mathcal{B}^{\mathrm{e.s.o}}_u,\ u \in \mathcal{U}^{\mathrm{TE}} \cup \mathcal{U}^{\mathrm{RE}},\ i \in \mathcal{I}. \tag{12}$$

4.4.2 Generation limits and reserves

For renewable generators, the power limits (maximum and minimum) are modeled as follows.

$$\beta_{u,i}\underline{g}_{u,i} \leq g_{u,i} \leq \beta_{u,i}\overline{g}_{u,i}, \qquad u \in \mathcal{U}^{\mathrm{RE}},\ i \in \mathcal{I}. \tag{13}$$

Concerning thermal generator in operation, the maximum power level should be equal or major to its output power, plus the sum of regulation reserve committed, plus 10-minute spinning reserve committed, plus 30-minute spinning reserve committed. If the generator is in start-up process, the sum should be equal or less to its minimal operative power.

$$g_{u,i} + rre_{u,i} + rro^{10}_{u,i} + rro^{30}_{u,i} \leq \beta_{u,i}\overline{g}_{u,i} + \beta^{s}_{u,i}\underline{g}_{u,i}, \qquad u \in \mathcal{U}^{\mathrm{TE}},\ i \in \mathcal{I}. \tag{14}$$

Regarding hydro generators, the maximum power level should be equal or major to its output power, plus the sum of regulation reserve committed, plus 10-minute spinning reserve committed, plus 30-minute spinning reserve committed.

$$g_{u,i} + rre_{u,i} + rro^{10}_{u,i} + rro^{30}_{u,i} \leq \beta_{u,i}\overline{g}_{u,i}, \qquad u \in \mathcal{U}^{\mathrm{HI}},\ i \in \mathcal{I}. \tag{15}$$

For both, hydro and thermal generators, their power level should be equal or less to the maximum level of the operating range selected ro. If the generator does not sell regulation reserve, its power level should be equal or less to the operating range selected. In case of selling regulation reserve ($\beta^{RE} = 1$) its power level plus its reserve regulation should be equal or less to the maximum limit of reserve regulation for the operating range selected.

$$g_{u,i} + rre_{u,i} \leq \sum_{ro \in \mathcal{RO}_u} \{\beta^{RO}_{u,ro,i}\overline{g}^{RO}_{u,ro} + \beta^{RE}_{u,ro,i}(\overline{g}^{RE}_{u,ro,i} - \overline{g}^{RO}_{u,ro})\}, \qquad u \in \mathcal{U}^{\mathrm{TE}} \cup \mathcal{U}^{\mathrm{HI}},\ i \in \mathcal{I}. \tag{16}$$

In order to commit a generator for supplying regulation reserve an generation operative range $\mathcal{RO}$ should be selected.

$$\beta^{RE}_{u,ro,i} \leq \beta^{RO}_{u,ro,i}, \qquad ro \in \mathcal{RO}_u; u \in \mathcal{U}^{\mathrm{TE}} \cup \mathcal{U}^{\mathrm{HI}},\ i \in \mathcal{I}. \tag{17}$$

Concerning hydro generators, their power level should be equal or major to the minimum level of the operating range selected ro. If the generator does not sell regulation reserve, its power level should be equal or major to the minimum level of the operating range selected. In case of selling regulation reserve ($\beta^{RE} = 1$) its power level minus its reserve regulation should be equal or major to the minimum limit of reserve regulation for the operating range selected.

$$g_{u,i} - rre_{u,i} \geq \sum_{ro \in \mathcal{RO}_u} \{\beta^{RO}_{u,ro,i}\underline{g}^{RO}_{u,ro} + \beta^{RE}_{u,ro,i}(\underline{g}^{RE}_{u,ro,i} - \underline{g}^{RO}_{u,ro})\}, \qquad u \in \mathcal{U}^{\mathrm{HI}},\ i \in \mathcal{I}. \tag{18}$$

With regard of thermal generators, their power level should be equal or major to the minimum level of the operating range selected ro. If the generator does not sell regulation reserve, its power level should be equal or major to the minimum level of the operating range selected plus the synchronous power (start-up power of a generator). In case of commit of selling regulation reserve

($\beta^{RE} = 1$) its power level minus its reserve regulation should be equal or major to the minimum limit of reserve regulation for the operating range selected plus the synchronizing power.

$$g_{u,i} - rre_{u,i} \geq \sum_{ro \in \mathcal{RO}_u} \{\beta^{RO}_{u,ro,i} \underline{g}^{RO}_{u,ro} + \beta^{RE}_{u,ro,i}(\underline{g}^{RE}_{u,ro,i} - \underline{g}^{RO}_{u,ro})\} + \beta^{s}_{u,i} g^{sync}_{u,i}, \qquad u \in \mathcal{U}^{\mathrm{TE}},\ i \in \mathcal{I}. \quad (19)$$

Synchronizing power is the power level a generator provide once it is connected and has the same system frequency.

4.4.3 Reserve limits and ramps

The 10-minute spinning reserve limit should be within the operative limits.

$$0 \leq rro^{10}_{u,i} \leq \beta_{u,i} \overline{RRo}^{10}_{u,i}, \qquad u \in \mathcal{U}^{\mathrm{TE}} \cup \mathcal{U}^{\mathrm{HI}},\ i \in \mathcal{I}. \quad (20)$$

The 30-minute spinning reserve limit should be within the operative limits.

$$0 \leq rro^{30}_{u,i} \leq \beta_{u,i} \overline{RRo}^{30}_{u,i}, \qquad u \in \mathcal{U}^{\mathrm{TE}} \cup \mathcal{U}^{\mathrm{HI}},\ i \in \mathcal{I}. \quad (21)$$

The regulation reserve limit should be within the operative limits.

$$\sum_{ro \in \mathcal{RO}_u} \beta^{RE}_{u,ro,i} Mrre_{u,i} \leq rre_{u,i} \leq \sum_{ro \in \mathcal{RO}_u} \beta^{RE}_{u,ro,i} \overline{RRe}_{u,ro,i}, \qquad u \in \mathcal{U}^{\mathrm{TE}} \cup \mathcal{U}^{\mathrm{HI}},\ i \in \mathcal{I}. \quad (22)$$

The 10-minute non-spinning reserve limit should be within the limits are modeled as follows.

$$0 \leq rnr^{10}_{u,i} \leq (1 - \beta^{s}_{u,i} - \beta_{u,i}) RNR^{10}_{u,i}, \qquad u \in \mathcal{U}^{\mathrm{TE}},\ i \in \mathcal{I}. \quad (23)$$

$$0 \leq rnr^{10}_{u,i} \leq (1 - \beta_{u,i}) RNR^{10}_{u,i}, \qquad u \in \mathcal{U}^{\mathrm{HI}},\ i \in \mathcal{I}. \quad (24)$$

The 30-minute non-spinning reserve limit should be within the limits are modeled as follows.

$$0 \leq rnr^{30}_{u,i} \leq (1 - \beta^{s}_{u,i} - \beta_{u,i}) RNR^{30}_{u,i}, \qquad u \in \mathcal{U}^{\mathrm{TE}},\ i \in \mathcal{I}. \quad (25)$$

$$0 \leq rnr^{30}_{u,i} \leq (1 - \beta_{u,i}) RNR^{30}_{u,i}, \qquad u \in \mathcal{U}^{\mathrm{HI}},\ i \in \mathcal{I}. \quad (26)$$

4.4.4 Ramp up/down

The power increase in generators between two consecutive time intervals or ramp-up rate in thermal and hydro generators.

$$g_{u,i} - g_{u,i-1} \leq RS_u, \qquad u \in \mathcal{U}^{\mathrm{TE}} \cup \mathcal{U}^{\mathrm{HI}},\, i \in \mathcal{I}. \tag{27}$$

The power reduction in generators between two consecutive time intervals or ramp-down rate in thermal and hydro generators.

$$g_{u,i-1} - g_{u,i} \leq RB_u + \tau_{u,i}(\overline{g}_{u,i-1} - RB_u) \qquad u \in \mathcal{U}^{\mathrm{TE}} \cup \mathcal{U}^{\mathrm{HI}},\, i \in \mathcal{I}. \tag{28}$$

The power increase in generators in start-up processes between two consecutive time intervals or starting-up ramp in hydro generators are modeled as follows.

$$gs_{u,i} - gs_{u,i-1} \leq g_u^{sync}(\beta^s_{u,i} - \beta^s_{u,i-1}) + RS_u^{sync}\beta^s_{u,i-1}, \qquad u \in \mathcal{U}^{\mathrm{TE}},\, i \in \mathcal{I}. \tag{29}$$

$$gs_{u,i} - gs_{u,i-1} \geq RS_u^{sync}\beta^s_{u,i-1} - \underline{g}_{u,i}\beta_{u,i}, \qquad u \in \mathcal{U}^{\mathrm{TE}},\, i \in \mathcal{I}. \tag{30}$$

4.4.5 Minimum up and down time

Once a generator is turned on, it will be kept on at least a minimum number of time intervals before turning it off.

$$\sum_{i'=i+ts_u}^{i+ts_u+\bar{t}_u} \beta_{u,i'} - \bar{t}_u\alpha_{u,i} \geq 0, \qquad u \in \mathcal{U}^{\mathrm{TE}} \cup \mathcal{U}^{\mathrm{HI}},\, i, i' \in \mathcal{I}. \tag{31}$$

Once a generator is turned off, it will be kept off at least a minimum number of time intervals before turning it on.

$$\sum_{i'=i}^{i+\underline{t}_u-1} \beta_{u,i'} + \underline{t}_u\tau_{u,i} \leq \underline{t}_u, \qquad u \in \mathcal{U}^{\mathrm{TE}} \cup \mathcal{U}^{\mathrm{HI}},\, i, i' \in \mathcal{I}. \tag{32}$$

4.4.6 Variable startup costs

The following constraints are based on reference Morales-España et al. [28]. Constraints (33) and (34) establish the relationship between the number of hours that the generator has been disconnected and its corresponding segment in the startup costs function for the current interval.

These constraints assure that the number of hours that the generator will be disconnected are within the interval of the startup segment delimited between $[\underline{T}_{u,s}, \overline{T}_{u,s})$.

$$sa_{u,i,s} \leq \sum_{i' \in \mathcal{I}'_i} \tau_{u,i'}, \qquad u \in \mathcal{U}^{\mathrm{TE}},\ i \in \mathcal{I},\ s \in \mathcal{S} - \{|\mathcal{S}|\}, \tag{33}$$

where

$$\mathcal{I}'_i = \{i' | i - \overline{T}_{u,s} + 1 \leq i' \leq i - \underline{T}_{u,s}, 0 < i' < i\} \tag{34}$$

.

The relationship between the start-up segments and the start-up variables is modeled as follows.

$$\alpha_{u,i} \leq \sum_{s \in \mathcal{S}} sa_{u,i,s}, \qquad u \in \mathcal{U}^{\mathrm{TE}},\ i \in \mathcal{I}, \tag{35}$$

4.5 Hydraulic constraints

4.5.1 Energy limits on reservoirs

Reservoirs water volume should be kept within the minimum and maximum storage operative limits.

$$\underline{w}_e \leq w_{e,i} \leq \overline{w}_e, \qquad e \in \mathcal{E},\ i \in \mathcal{I} \tag{36}$$

4.5.2 Hydraulic balance

The reservoir water volume in an time interval i amounts to: the water volume stored in the previous time interval $i-1$; plus generators turbine water discharge in reservoirs upstream; minus turbine water discharge of generators linked to the reservoirs. Evidently, the water balance equation integrates natural inflows, different uses of water unrelated to energy generation, water spillage in the reservoirs, water spillage in the upstream reservoirs. In all cases travel time delays are taken into account.

$$\begin{aligned} w_{e,i} = & w_{e,i-1} + \sum_{v \in \mathcal{V}^{\mathrm{c}}_e} \sum_{u \in \mathcal{HI}_v} M q_{u,i-\delta_v} - \sum_{v \in \mathcal{V}^{\mathrm{r}}_e} \sum_{u \in \mathcal{HI}_v} M q_{u,i} \\ & + \epsilon_{e,i} - \rho_{e,i} - \sum_{v \in \mathcal{V}^{\mathrm{r}}_e} \kappa_{v,i} + \sum_{v \in \mathcal{V}^{\mathrm{c}}_e} \kappa_{v,i-\delta_v}, \qquad e \in \mathcal{E},\ i \in \mathcal{I}. \end{aligned} \tag{37}$$

Figure 1 represents the water balance in a reservoir. The water inputs to the reservoir is represented by the natural inflow minus other uses, plus by the water comes from the reservoir upstream. The water output from the reservoir to the river is the sum of the discharge of water that passes through turbines plus the discharge of water, which is not used to generate electricity. The sum of water discharge passing trough turbines of generators linked to a reservoir should meet

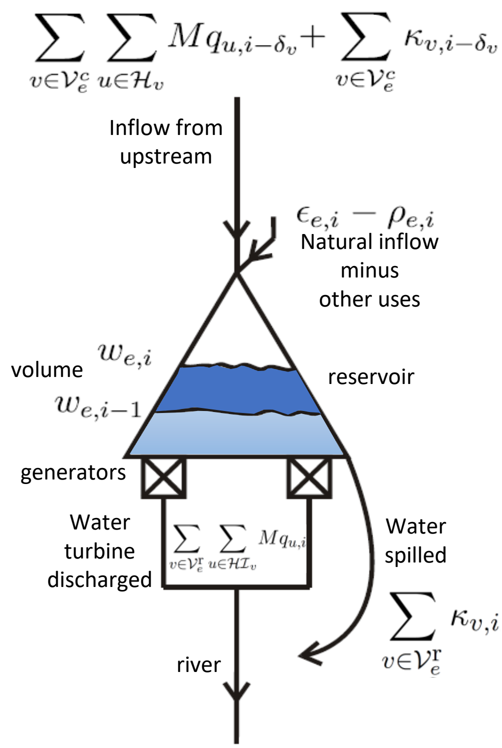

Figure 1: Hydro balance in reservoirs.

minimum and maximum limits in the divergent river channel.

$$\underline{Q}_{v,i} \leq \sum_{u\in\mathcal{HI}_v} q_{u,i} \leq \overline{Q}_{v,i}, \qquad v \in \mathcal{V}_e^{\mathrm{r}}, e \in \mathcal{E} \tag{38}$$

For each hydro generator, the water discharge passing trough turbine in reservoirs should meet minimum and maximum limits.

$$\beta_{u,i}\underline{q}_{u,i} \leq q_{u,i} \leq \beta_{u,i}\overline{q}_{u,i}, \qquad u \in \mathcal{U}^{\mathrm{HI}},\ i \in \mathcal{I}. \tag{39}$$

4.5.3 Hydraulic generation

Hydro generation power depends quadratically on turbine water discharge rate and quadratically on the reservoir head. The function used here is known as Glimn-Kirchmayer [21]. The constraint below is known as hydro power function (HPF). Its parameters $a_{1,u}, b_{1,u}, c_{1,u}, a_{2,u}, b_{2,u}, c_{2,u}, a_{3,u}, b_{3,u}, c_{3,u}$ depend on the reservoir design, turbine and generator features. Those parameters are obtained through several tests in each hydroelectric plant.

$$g_{u,i} = \beta_{u,i}\big((a_{1,u} + b_{1,u}h_{v,i} + c_{1,u}h_{v,i}^2) + (a_{2,u} + b_{2,u}h_{v,i} + c_{2,u}h_{v,i}^2)q_{u,i}$$

$$+ (a_{3,u} + b_{3,u}h_{v,i} + c_{3,u}h_{v,i}^2)q_{u,i}^2\big), \qquad u \in \mathcal{HI}_v,\ v \in \mathcal{V}_e^{\mathrm{r}},\ e \in \mathcal{E},\ i \in \mathcal{I} \tag{40}$$

The value of the effective hydraulic head $h_{v,i}$ is calculated with the height of forebay water (above the hydroelectric dam wall) minus the tailwater level (below the hydroelectric dam wall) minus the head losses that occur due to friction in pipes. Thus, the constraint 41 calculates the $h_{v,i}$ where $\omega()$ represents a function with an input volume and an output forebay height and it is often non-linear; $\mu()$ represents a function with an input water discharge and an output tailwater level; $\zeta()$ is a function with an input water discharge and an output the head losses. These functions depend on each reservoir's design; therefore, $\omega()$, $\mu()$, and $\zeta()$ are written generically.

$$h_{v,i} = \omega(w_{e,i-1}) - \mu\left(\sum_{u\in\mathcal{H}_v} q_{u,i}\right) - \sum_{u\in\mathcal{H}_v} \zeta(q_{u,i}), \qquad v \in \mathcal{V}_e^r,\ e \in \mathcal{E},\ i \in \mathcal{I}, \tag{41}$$

The non-linear feature of the hydro power function constraint requires an approximation method to be successfully integrated in a MILP. The method used in this work is the approximation to Taylor polynomial. This method generates an alternative constraint to replace the former (40).

4.6 Network constraints

4.6.1 Power flow limits

The power flow in a transmission tie-line is modeled as follows.

$$f_{br,i} = \sum_{n\in\mathcal{N}} PTDF_{br,n,i}\, iny_{n,i}, \qquad br \in \mathcal{BR},\ i \in \mathcal{I}. \tag{42}$$

where $f_{br,i}$ represent the power flow in a transmission tie-line br which depends on parameters $PTDF_{br,n,i}$ and the power injection $iny_{n,i}$ for each bus n for each period i.

A detailed description of the calculation of those PTDF is explained by Hinojosa-Mateus et al. [18] and Tejada-Arango et al. [35].

The following constraint fixes the maximum limits of flow and counterflow power in tie-line br.

$$\overline{fn}_{br,i} \leq f_{br,i} \leq \overline{fp}_{br,i} \qquad i \in \mathcal{I}. \tag{43}$$

4.6.2 Transmission losses

The losses in the system are calculated using the following constraint.

$$Loss_i = \sum_{br\in\mathcal{BR}} R_{br}(f_{br,i})^2 \qquad i \in \mathcal{I}. \tag{44}$$

The non-linear feature of this constraint requires an approximation method to be successfully integrated in a MILP. The method used in this work is tangent planes. This method generates an set of alternative constraints to replace the former (44).

4.7 Logical constraints

The shift between commitment orders (starting-up, synchronizing, operating and shutting-down) are modeled as follows:

A generator cannot start up and shut down at the same time.

$$\alpha_{u,i} + \tau_{u,i} \leq 1 \qquad u \in \mathcal{U}^{\mathrm{TE}} \cup \mathcal{U}^{\mathrm{HI}},\, i \in \mathcal{I}. \tag{45}$$

A hydro generator cannot start up and shut down and operate (to provide energy in stable fashion within its operative limits) at the same time.

$$\beta_{u,i} - \beta_{u,i-1} - \alpha_{u,i} + \tau_{u,i} = 0, \qquad u \in \mathcal{U}^{\mathrm{HI}},\, i \in \mathcal{I}. \tag{46}$$

A thermal generator cannot synchronize, start up, shut down and operate (to provide energy in stable fashion within its operative limits) at the same time.

$$\beta_{u,i} - \beta_{u,i-1} - \alpha_{u,i} + \tau_{u,i} + \beta^{s}_{u,i} - \beta^{s}_{u,i-1} = 0, \qquad u \in \mathcal{U}^{\mathrm{TE}},\, i \in \mathcal{I}. \tag{47}$$

To activate a generator operative range, the unit should be committed for operation.

$$\sum_{ro \in \mathcal{RO}_u} \beta^{RO}_{u,ro,i} = \beta_{u,i}, \qquad u \in \mathcal{U}^{\mathrm{TE}} \cup \mathcal{U}^{\mathrm{HI}},\, i \in \mathcal{I}. \tag{48}$$

A generator can start up only if it was off in the previous time interval.

$$\beta_{u,i-1} + \beta^{s}_{u,i} \leq 1, \qquad u \in \mathcal{U}^{\mathrm{TE}},\, i \in \mathcal{I}. \tag{49}$$

A generator is not committed for operation during the starting-up time intervals.

$$\sum_{i'=i}^{i+ts_u-1} \beta_{u,i'} + ts_u \alpha_{u,i} \leq ts_u, \qquad u \in \mathcal{U}^{\mathrm{TE}},\, i \in \mathcal{I}. \tag{50}$$

A generator is committed for the starting-up process during the starting-up time intervals.

$$\sum_{i'=i}^{i+ts_u-1} \beta^{s}_{u,i'} - ts_u \alpha_{u,i} \geq 0, \qquad u \in \mathcal{U}^{\mathrm{TE}},\, i \in \mathcal{I}. \tag{51}$$

Generators power during the starting-up process should be kept within a minimum limit given by its synchronizing power and a maximum limit given by its minimum operative power.

$$\beta^{s}_{u,i} g^{sync}_{u} \leq gs_{u,i} \leq \beta^{s}_{u,i} \underline{g}_{u,i}, \qquad u \in \mathcal{U}^{\mathrm{TE}},\ i \in \mathcal{I}. \tag{52}$$

4.8 Additional constraints

This constraints distributes the net regulating reserve among different generators aiming to provide more reliability in the system.

$$\sum_{u \in r} \sum_{ro \in \mathcal{RO}} \beta^{re}_{u,ro,i} \geq N_i, \qquad i \in \mathcal{I}. \tag{53}$$

The number of shutdowns for a generator during the day cannot be more than the established limit.

$$\sum_{i \in \mathcal{I}} \tau_{u,i} \leq \overline{NP}_u, \qquad u \in \mathcal{U}^{\mathrm{TE}} \cup \mathcal{U}^{\mathrm{HI}}. \tag{54}$$

5 Solution method

The model posed in Section 4 has continuous and binary variables and some non-linear components such as the HPF (40) and the transmission losses (44). It also incorporates power flow constraints in the network. Those constraints keep the power flow within safe limits. A typical real-world instance of this problem has more than 7000 buses, 8000 lines, and 400 generators. A consequence of this is that including, simultaneously, all the transmission constraints may lead to high solution times when attempting to solve the model. Due to this complexity, in a typical solution strategy, the (44) constraints are relaxed and are incorporated into the model as violations are being found.

A common way to solve this type of UCP integer programming model has been through decomposition algorithms [22, 13]. This technique, as depicted in Figure 2, works as follows.

The master problem (MP) is formed by minimizing (1) subject to (2) to (39), (45) to (54) and (57); it is solved to find out the generators' schedule, that is. In other words, it aims to determine both which generators should be turned on and off and how much power should they produce.

The MP solution is the generation schedule. The status of generators is fixed and sent to the SP, which calculates the power flow in the lines using the DC Power Flow method. With those results, possible violations of network constraints (43) can be identified with a feasibility test. These violations or cuts are added back to the model and passed back to the MP. Moreover, constraint (42) that represents the power flow in the violated tie-lines is added too. Some examples of these approaches are Marín-Cano et al. [23], dos Santos and Diniz [12].

Constraints (44) consider the losses in the system. However, they are non-linear and cannot be added directly to a linear master problem. Therefore, the Tangential Approximation Method

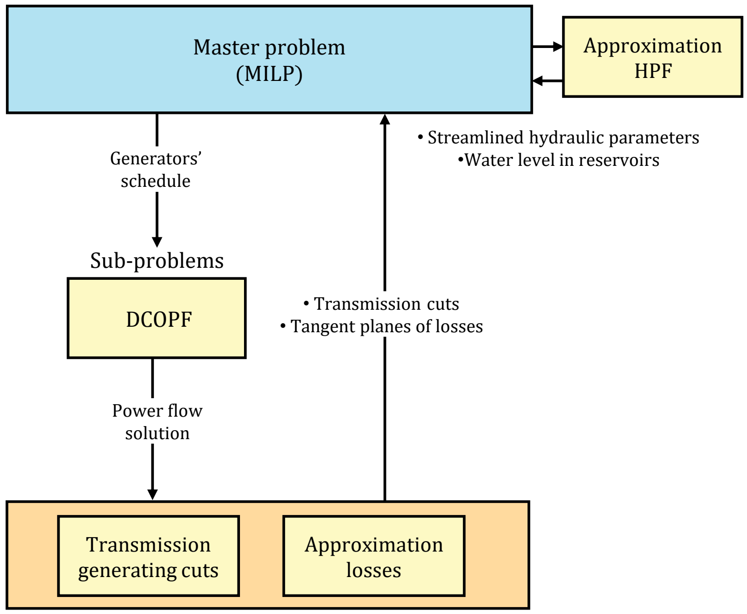

Figure 2: Iterative decomposition method, based on [14].

developed by Geoffrion [16] is used to tackle its non-linearity. Notably, its application in the market in Mexico is widely documented in Félix [14]. The constraints (tangential planes) have the following mathematical structure: (55):

$$Loss_i - \sum_{n \in \mathcal{N}} LSF_{n,i}^{k-1} iny_{n,i} \geq Loss_i^{SP} - \sum_{n \in \mathcal{N}} LSF_{n,i}^{k-1} iny_{n,i}^{k-1}, \qquad i \in \mathcal{I}. \tag{55}$$

The variable $Loss_i^{SP}$ determines the exact losses in the network obtained from substituting the power flow in the Equation (44). Unlike the variable $Loss_i^{SP}$, $Loss_i$ is a variable, in the MP, that approximates the sum of losses in the system.

The loss sensitivity factors parameters $LSF_{n,i}^{k-1}$ represent the variation in losses in the system when modifying a power unit in each node. The parameters $LSF_{n,i}^{k-1}$ are calculated at the end of each iteration k and are expressed in the following equation:

$$LSF_{n,i}^{k-1} = \frac{\partial Loss_i}{\partial iny_{n,i}}|_{iny_{n,i}=iny_{n,i}^{k-1}}, \qquad n \in \mathcal{N},\, i \in \mathcal{I},\, k \geq 1. \tag{56}$$

Equation (56) is solved numerically and parameters $LSF_{n,i}^{k-1}$ are used to build a new set of constraints (55). The theory of Sensitivity Transmission Loss Factors used in this work is based on [24].

A decomposition approach such as the one presented in this paper is widely used to plan the operation of real-life power systems. However, in this work, a new component has been added to deal with the non-linear characteristics of HPF using the approximation of the first-order Taylor polynomial. The method provides the constraint (57) that replaces (40) in the MP. The procedure for obtaining this constraint and its parameters $QW_{u,e,i}, Q_{u,e,i}, W_{u,e,i}$ are explained in Appendix C.

$$g_{u,i} \leq \beta_{u,i} QW_{u,e,i} + Q_{u,e,i} q_{u,i} + W_{u,e,i} w_{e,i}, \qquad u \in \mathcal{HI}_e,\, e \in \mathcal{E},\, i \in \mathcal{I} \tag{57}$$

Description of algorithm

The proposed method in this work is outlined in Algorithm 1.

This algorithm begins by solving the MP in step six that uses a branch-and-bound method. It is worth-nothing, that in the first version, the MP does not include transmission losses (tangential planes) nor any transmission constraints (cuts). The solution is saved in X that contains the value of all the decision variables of the MP.

An iterative process begins and runs until the stopping criteria are met. There are two conditions for stopping. The first is when the relative error in approximation losses ($ErrLosses$) is greater or equal to the given tolerance ($tolerance$). The second one is the absence of violations of the safe transmission limits.

Within the loop, the method SolvingSP() that consist of solving a series of SPs using DC Power Flow method is run, one for each period i. The power flow in the lines (F) is calculated by using the information of the injections in nodes and the topology of the network, based on the results from the SP.

Then, GeneratingCuts() identifies violations to the safe limits in lines (if any) and generates the cuts: (42) and (43). The cuts are added to the MP using AddingCuts(). The exact losses are calculated using (44) and are registered in $Loss_i^{SP}$. Then AddingTangentPlanes() generates the tangent planes of losses with the structure 55. Subsequently, the tangent planes are added to the MP. After this, MP is solved again considering losses and safe limits in the tie-lines.

Then, the maximum relative error in the estimated losses in all periods i is calculated and registered in ($ErrLosses$). The value of the variable $Loss_i$ is obtained from the MP.

Finally, the parameters $LSF_{n,i}^k$ are updated with 56 by using the new transmission losses in the lines $Loss_{SP}^k$ and the new injections in the nodes $iny_{n,i}^k$.

When there are no more violations in the safe limits of the transmission and a loss tolerance is reached, the algorithm stops.

Algorithm 1 Iterative method employed

Input: P:=Instance of the problem, *tolerance*

Output: X^{*}:=An optimal solution to the problem

$k \leftarrow 1$
$Lossi^{SP} \leftarrow 0$
$LSF^{k-1}n, i \leftarrow 0$
$Errlosses \leftarrow \infty$ {Relative difference of the losses between approximated and exact losses}
Cuts $\leftarrow \phi$ {Set of transmission cuts}
$X \leftarrow$ SolvingMP()
while ($Errlosses \geq tolerance$) or (Cuts $\neq \phi$) **do**
    Cuts $\leftarrow \phi$
    F $\leftarrow$ SolvingSP(X) {Power flow in lines}
    Cuts $\leftarrow$ GeneratingCuts(F)
    if Cuts $\neq \phi$ **then**
        MP $\leftarrow$ AddingCuts(MP,Cuts)
    end if
    $Loss^{SP}i \leftarrow$ CalculatingLosses(F)
    MP $\leftarrow$ AddingTangentPlanes(MP, $LSF^{k-1}n, i$, $Loss_{i}^{SP}$)
    $X \leftarrow$ SolvingMP()
    $Errlosses \leftarrow \max((Loss_i - Loss_i^{SP})/Loss_i), \forall i \in \mathcal{I}$
    $LSF^{k}n, i \leftarrow$ updatingLSF()
    $k \leftarrow k + 1$
end while
return X^{*}

6 Experimental work

For evaluating the performance of the model and the method employed in this work two different sets of experiments are carried out. The first set consists of solving a representative instance of DAM for the Central Interconnected System (CIS) which is the largest and most complex system in Mexico. A representation of the CIS is displayed in Figure 3.

The first aim of this experiment is to analyze the results of both the decision variables and market behavior in terms of commitment and dispatch of generators, energy balance in basins, water level changes and energy generated in reservoirs, market participant's profits, and energy prices for each node.

The second set of experiments revolve around solving multiple instances created from to publicly available information of DAM in Mexico. The main aim is to evaluate the performance of the

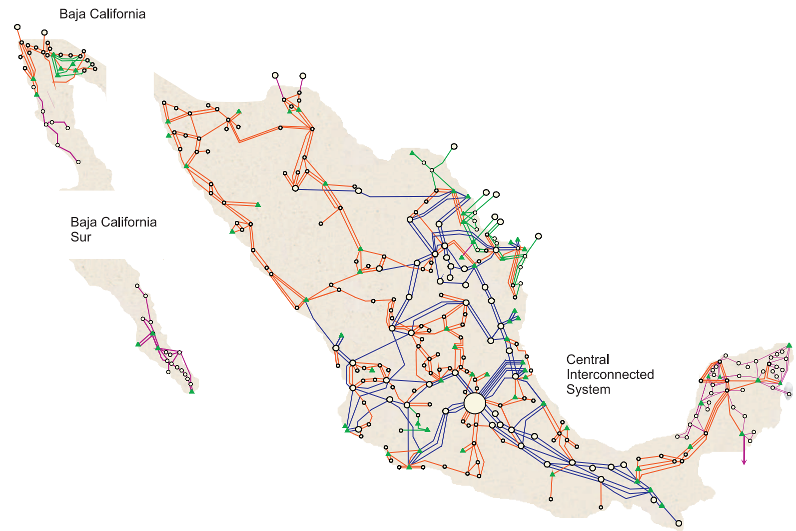

Figure 3: Central Interconnected System in Mexico.

proposed model and methods in terms of time for execution, number of iterations between the MP and the SPs, number of transmission cuts added by the SP and the approximation losses tolerance.

The model and method were coded with Intel Fortran and C++ languages using the Intel oneAPI DPC++/C++ version 2020. Fortran is used to form the MP optimization problem and solve the SPs. C++ is used as a link between the Fortran and the solver. The solver used was 64-bit based IBM-CPLEX 12.10 with optimality gap of 0.0001%. The hardware employed in all tests was a 64-bit with 16GB of RAM with an Intel(R) Xeon(R) CPU E3-1240 v3 @ 3.40GHz.

6.1 Experiment 1: A case study

This section presents a case study that outlines the model. This instance was obtained from the ISO in Mexico with data from the electrical market. The elements modeled in the CIS power system are shown in Table 1.

Table 1: Power system dimensions

Intervals	24
Thermal units	217
Hydroelectric units	63
River basins	8
Renewable units	16
Tie-lines	85
Reserves zones	4
Loads	6222
Buses	7062
Lines	8000
Reservoirs	16

The model has 24 intervals, around 436,103 variables (408,467 are continuous and whilst 27,636 are binary) and 141,671 constraints. Figure 4 shows the expected load demand of the instance and the energy price component or dual variables of the power balance constraints. The load demand varies from 30,000 to 38,000 MW whilst the prices vary from 1,000.0$/MW to 1,900 $/MW. As it is shown in Figure 4, the prices follow the expected demand trend; so the higher the demand goes, the higher the prices get.

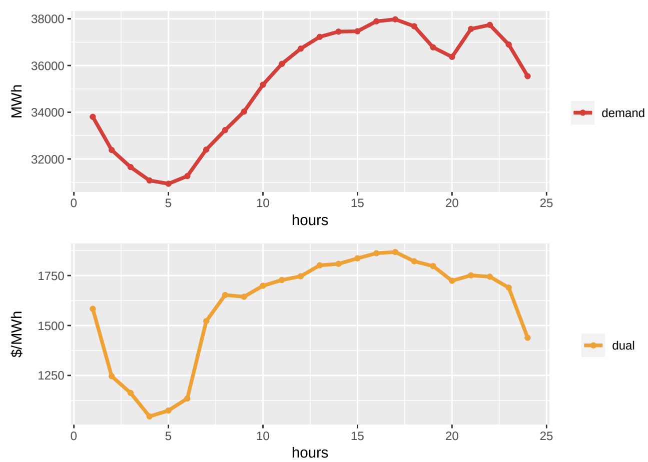

Figure 4: Expected load demand and energy prices.

As it is shown in Figure 5 the transmission losses are estimated after iteration one in the MP. After iteration two, the estimation is more precise in comparison to the one calculated by the SPs. After each iteration the estimation of losses gradually improves, as shown in the Figure 5.

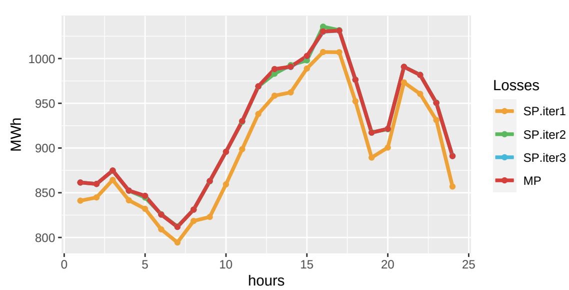

Figure 5: Transmission losses after first iteration.

Figure 6 shows the net hydraulic head and water discharged for a representative reservoir. It can be seen that the amount of water discharged for a hydroelectric unit depends on the net hydraulic head of its reservoir, thus the highest the head is located less water is required to produce energy.

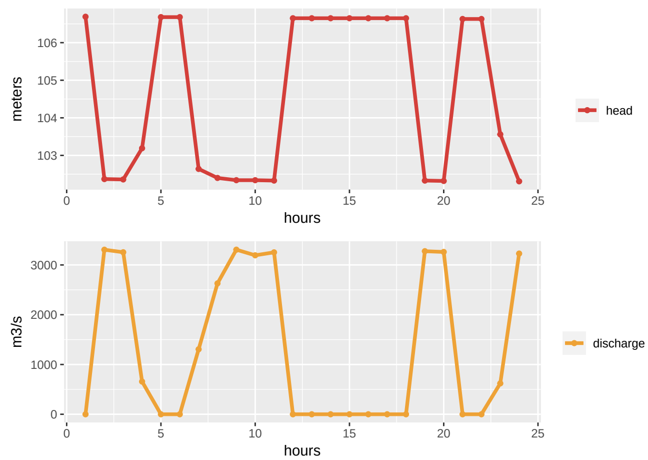

Figure 6: Net hydraulic head and water discharged.

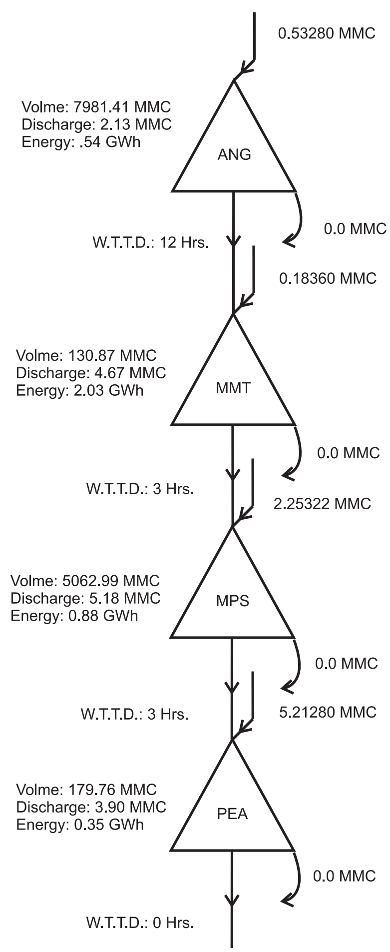

Figure 7: Grijalva river basin, hour fourteen.

Figure 7 represents the water balance flow in a river basin called *Grijalva*. The water volume held at the *Malpaso* reservoir (MPS) is 5,062.99 MMC at hour fourteen. At hour thirteen, the MPS reservoir held 5,065.92 MMC. The net water inflow to the MPS reservoir is the sum of its natural water inflow at hour fourteen, 0.2628 MMC, plus the water discharged of the *Chicoasén* (MMT) reservoir at hour eleven, 1.99042 MMC, amounting to 2.25322 MMC. The small difference in water balance is explained because there is a water time travel delay of three hours between the MPS and the MMT reservoirs. The water discharged at hour fourteen of MPS is 5.18 MMC. Therefore, the volume at hour fourteen held at MPS is the sum of the volume of the previous hour plus the net inflow for the current hour minus the water discharged for the current hour, that is $5,065.92 + 2.25322 - 5.18 = 5,062.99$ MMC.

Also, three iterations were sufficient to estimate the relative error in losses $Errlosses$ at 0.001%.

6.2 Experiment II: Performance tests

The goal of this experiment is to test the performance of the model in other real-world instances using the CIS energy system of the electricity market in Mexico. The tests were carried out with four instance groups called MEM1, MEM2, MEM3 and MEM4. Each group has 80 instances were created from publicly available information of Wholesale Electricity Market (WEM) in Mexico. The original instances were modified by randomly choosing a percentage (70%, 80%, 90%, 95%) of all thermal generators, and both the demand, reserve requirements and generator bids were modified. The number of instances for each percentage are 20. The dimensions of each of the instances are shown in Table 2. MEM1 and MEM2 represent typical summer days, whereas MEM3 and MEM4 represent typical winter days. The load demand of each group is shown in Figure 8.

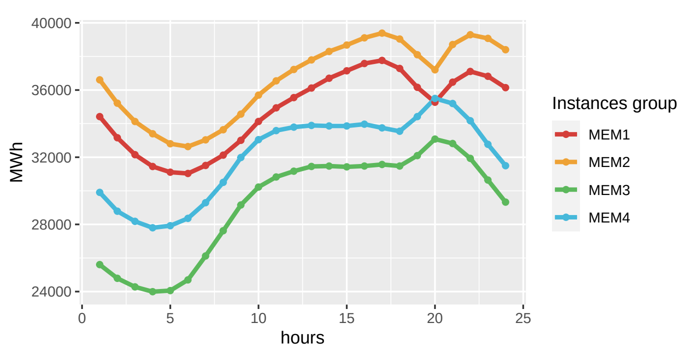

Figure 8: Summer and winter demands.

The key variables to measure and to analyse the performance of model are: average CPU time ($\bar{t}$); worst CPU time ($\bar{t^*}$); number of iterations (k) between the MP-SP until reaching the ($tolerance$); number of cuts ($nviol$) added by the SP (one for each tie-line violated); recorded loss error estimation ($Errlosses$). The instances were solved using a relative optimality gap of 0.0001%

Table 2: Instance size by data set.

	MEM1 summer	MEM2 summer	MEM3 winter	MEM4 winter
Intervals	24	24	24	24
Thermal units	255	255	253	253
Hydroelectric units	63	63	63	63
Renewable units	64	64	74	74
River basins	8	8	8	8
Tie-lines	89	88	106	105
Reserves zones	1	1	1	1
Loads	6054	6053	6077	6063
Buses	6553	6555	6605	6605
Lines	8519	8522	8581	8581
Reservoirs	16	16	16	16

and (*tolerance*) in the approximation losses tolerance of 0.005%. The problems are solved until they reach the time limit of 3500 seconds for each iteration or until they reach optimality. There is no time limit to solve the overall problem.

Table 3: Results for each instance.

instances	% *gen*	$\bar{t}$	t^*	k	k^*	$nviol$	$nviol^*$	$\overline{Errlosses}$	$\overline{profit}$
MEM1	70	8,593	24,573	3	5	17	25	0.0031	$1,880,824,498
	80	8,948	23,455	3	5	16	19	0.0030	$1,895,011,558
	90	14,375	29,437	3	4	17	20	0.0024	$1,910,265,699
	95	14,755	46,101	3	4	16	19	0.0026	$1,921,684,506
MEM2	70	4,829	20,534	3	4	9	12	0.0027	$2,141,180,824
	80	6,494	19,403	3	5	10	12	0.0028	$2,148,492,402
	90	6,362	19,112	3	3	10	12	0.0029	$2,167,144,875
	95	7,484	20,734	3	5	9	11	0.0025	$2,169,740,024
MEM3	70	4,632	18,493	5	7	14	19	0.0025	$20,044,116,952
	80	6,234	12,001	6	6	16	21	0.0028	$20,064,006,287
	90	9,779	22,156	6	8	13	19	0.0028	$20,091,123,339
	95	11,075	20,344	6	8	12	15	0.0028	$20,099,986,114
MEM4	70	1,952	5,107	4	7	8	13	0.0026	$20,476,495,913
	80	3,060	7,173	4	5	6	9	0.0024	$20,491,680,365
	90	9,873	26,767	4	7	7	9	0.0026	$20,516,227,967
	95	15,147	37,117	5	5	8	9	0.0023	$20,524,900,918

The results are outlined in Table 3. The column (*instances*) shows the names for each group of instances; the column (%) indicates the percentage of thermal generators selected that can be committed for each group of instances; the column (*gen*) enlists the number of generators that can be committed corresponding to the percentage; in the columns ($\bar{t}$) and (t^*) the CPU average time and the CPU maximum time used to solve the instances are registered. The columns ($\bar{k}$) and (k^*) display the median and maximum number of iterations between the MP and its SP for the instances in each row. The column (*nviol*) records the median number of tie-lines violated in the SP that generated transmission cuts in the MP. The column ($Err\bar{l}osses$) captures the average approximation loss reached. The column (*profit*) marks the average of economic profits in the market. All instances reached the approximation losses tolerance required and the MILP gap by the MP's.

It is worth noting that the rough number of iterations k is between two and seven, yet it is assumed that this figure is related to a higher number of generators in the system. Likely, the transmission losses wane and wax depending on the number of generators connected in the system.

The average error in estimating transmission losses in all instances is less than 0.005%; for instance, it represents a error of 0.00268% in an setting with maximum losses of 105.36 MW.

An expected result is the increase of CPU time when the instances are solved due to a higher percentage of generators. This rise is produced by the increased combinatorial complexity of the UCP model.

Another expected behavior is the decrease of profits with the rise in the generation offer caused by a higher number of generators in the system. This increment emulate a increasing competence in the market. With 95% of available generation, the economic profits nearly reach a minimum value.

Figures 9,10,11, and 12 have been designed to analyze the behavior of economic profits, CPU times, count of iterations between MP and SPs, and the number of family of transmission cuts added to the MP. On one hand, in the profit subfigure of Figures 9,10,11, and 12 the vertical axis represents the benefit of participant in millions of pesos. On the other hand, in the CPU time subfigure, the vertical axis represents the time of processing. For all Figures, the horizontal axis represents the percentage of thermal generators to be committed. The colored boxes represent 20 instances for each percent (70%,80%,90%,95%) for each group (MEM1, MEM2, MEM3, MEM4).

As it is observed in Table 2 and Figures 9,10,11, and 12, is shown a coherent behavior depicting a reduction of economic profits related with a higher number of generations in the system. Also, the results indicate that the more generators in the system, more CPU time required to process the data.

It is shown that the economic benefits increase gradually with the increment of generators in the system, since the instances resolved are more alike and closer to the 100 percent of units. This pattern matches normal expectations.

Furthermore, there is a gradual growth of CPU times while more generators are added into the system. This is a normal and expected pattern since a larger number of generators working entails more units to commit and a more complex problem to solve.

Finally, all instances used in this work and the individual results of each instance are available in the repository: `https://uanledu-my.sharepoint.com/:f:/g/personal/uriel_lezamaop_uanl_edu_mx/EsRr-9IX3_BMu-ImJBwEmSOBNyMxTPWV3cQELi6MJgDxcA?e=HhhNGb`.

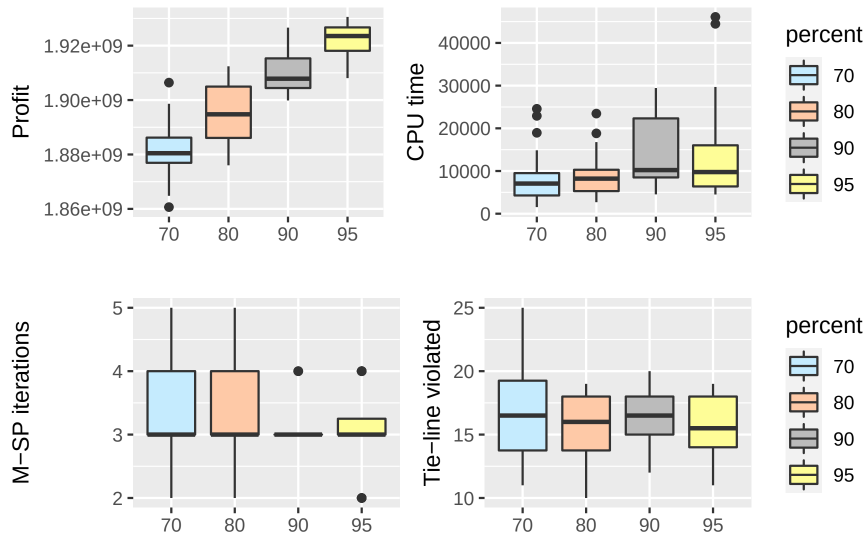

Figure 9: Results of the MEM1 instances.

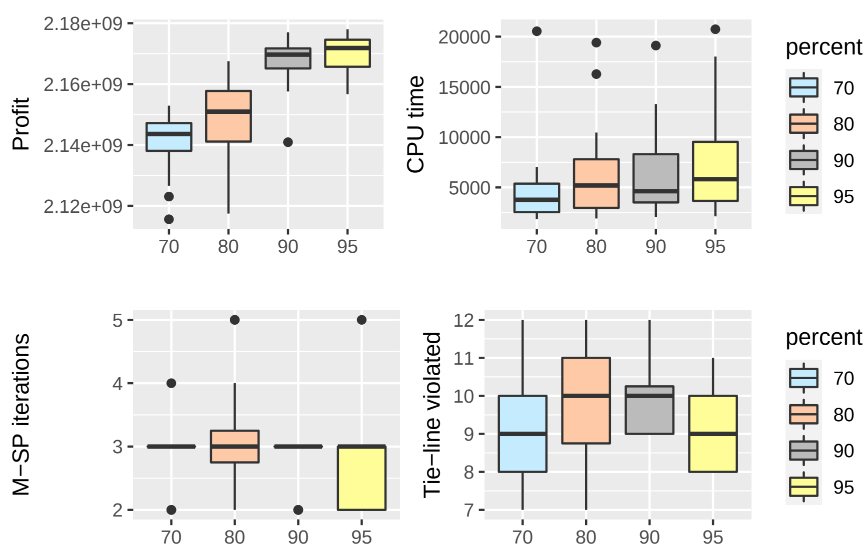

Figure 10: Results of the MEM2 instances.

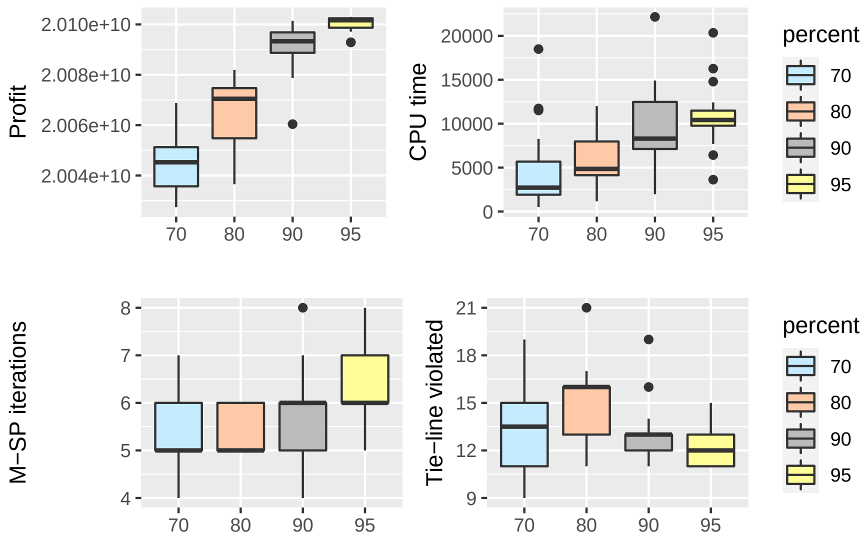

Figure 11: Results of the MEM3 instances.

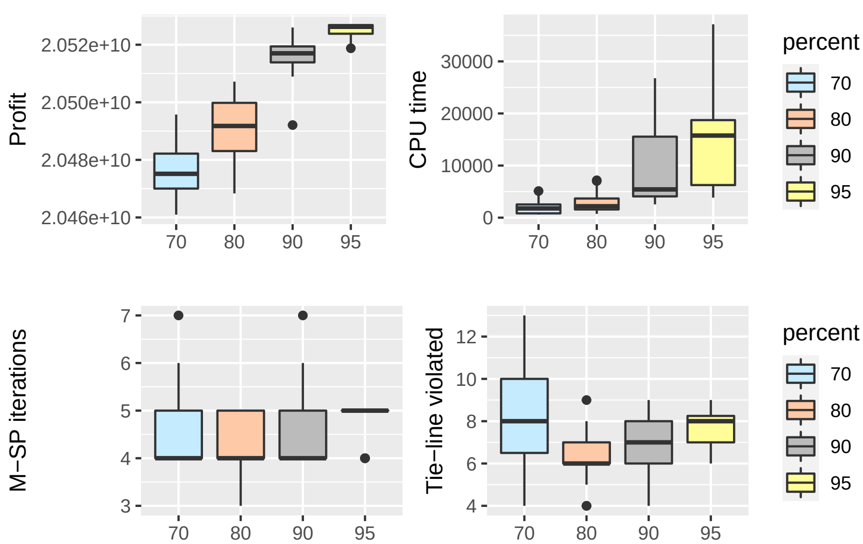

Figure 12: Results of the MEM4 instances.

7 Conclusions

This work demonstrates that the model and method proposed are useful to determine the generators production schedule in the day-ahead market. The model optimizes simultaneously energy and reserves and sets the maximum economic profit of the participants in such a market. The model incorporates all the essential real-life constraints such as prohibited operative zones, power flow limits in tie-lines, transmission losses, hydraulic generators and the balanced in the hydraulic network. In fact, the model provides an innovative solution to the problem of hydrothermal coordination. Finally, by incorporating five simultaneous reserves with different timing. This research shows a more comprehensive model than previous or similar ones.

The model consists of a large scale mixed-integer non-linear programming (MINLP). To deal with its non-linear feature several approximation methods were adopted to reduce it into a mixed-integer linear program (MILP). To tackle the approximation losses the tangential planes were used. Furthermore, the non-linear feature of the hydropower function was handled by using the Taylor series polynomial.

The method for determining the generation schedule consists of solving the MILP model several times in a decomposition approach by adding transmission constraints that are violated in the DC power flow subproblems. To achieve a better approximation in the hydro-generation calculation, the streamlining of the parameters in the approximation of HPF is carried out in each iteration.

Simulation results are presented on key representative instances of the wholesale electricity market in Mexico to demonstrate that the model is consistent and applicable to other markets that require hydrothermal coordination. Moreover, the results of the implementation process show that the solution times are adequate for operative purposes yet it is desirable and likely to reduce them even more for some complicated instances using a more tight and compact formulation.

As demonstrated in this research, the UCP models aids markets to obtain adequate solutions for scheduling operation generators and settles good financial arrangements to the participants in the market.

This work presents results projecting scenarios based on publicly available information from Mexico's ISO. They do not reflect nor represent the current workings of ISO but an theoretical model projecting patterns and calculations aiming to show how it could work. The instances used for this work were created from publicly available information and might not represent real operating scenarios. The comparisons have been done to assess the model performance with similar dimensions alike to the current system employed in Mexico.

Acknowledgments: The research of the first author was supported by a scholarship for graduate studies from the Mexican Council for Science and Technology CONACyT, by UANL (grant PAICYT CE1837-21), and by INEEL (grant FICYDET 220819-la-EXT-385). Moreover, the authors thank CENACE for providing data and discussing the usefulness of the model presented.

References

[1] I. Abdou and M. Tkiouat. Unit commitment problem in electrical power system: A literature review. *International Journal of Electrical and Computer Engineering*, 8(3):1357–1372, 2018.

[2] M. F. Anjos and A. J. Conejo. Unit commitment in electric energy systems. *Foundations and Trends in Electric Energy Systems*, 1(4):220–310, 2017.

[3] N. Babona and F. Rossell Pujós. Formulation of the short-term hydrothermal coordination of electricity generation and solutions through mixed integer programming. Technical Report DR 99/06, Universitat Politécnica de Catalunya, Barcelona, Spain, July 1999.

[4] S. Bisanovic, M. Hajro, and M. Dlakic. Hydrothermal self-scheduling problem in a day-ahead electricity market. *Electric Power Systems Research*, 78(9):1579–1596, 2008.

[5] S. Bisanovic, M. Hajro, and M. Dlajic. Mixed integer linear programming based thermal unit commitment problem in deregulated environment. *Journal of Electrical Systems*, 6(4):466–479, 2010.

[6] J. P. S. Catalão, H. M. I. Pousinho, and V. M. F. Mendes. Scheduling of head-dependent cascaded hydro systems: Mixed-integer quadratic approach. *Energy Conversion and Management*, 51(3):524–530, 2010.

[7] J L. Ceciliano-Meza, J. Álvarez López, A. De la Torre Sánchez, R. Nieva Gómez, I. Guillém Moya, R. Navarro Pérez, F. Perales Martínez, C. Torres Ruiz, A. Sánchez Sánchez, and M. B. Yildirim. Power system operator in Mexico reveals millions in savings by updating its short-term thermal unit commitment model. *Interfaces*, 46(6):493–502, 2016.

[8] J. H. Chow, W. De Mello, and K. W. Cheung. Electricity market design: An integrated approach to reliability assurance. *Proceedings of the IEEE*, 93(11):1956–1969, 2005.

[9] A. J. Conejo, J. M. Arroyo, J. Contreras, and F. A. Villamor. Self-scheduling of a hydro producer in a pool-based electricity market. *IEEE Transactions on Power Systems*, 17(4): 1265–1272, 2002.

[10] H. Daneshi, A. L. Choobbari, M. Shahidehpour, and Zuyi Li. Mixed integer programming method to solve security constrained unit commitment with restricted operating zone limits. In *2008 IEEE International Conference on Electro/Information Technology*, pages 187–192, Ames, USA, May 2008.

[11] A. L. Diniz and T. M. Souza. Short-term hydrothermal dispatch with river-level and routing constraints. *IEEE Transactions on Power Systems*, 29(5):2427–2435, 2014.

[12] T. N. dos Santos and A. L. Diniz. A dynamic piecewise linear model for DC transmission losses in optimal scheduling problems. *IEEE Transactions on Power Systems*, 26(2):508–519, 2011.

[13] S. M. Ezzati, G. R. Yousefi, M. M. Pedram, and M. Baghdadi. Security-constrained unit commitment based on hybrid benders decomposition and mixed integer non-linear programming. In *IEEE International Energy Conference*, pages 233–237, Manama, Bahrain, December 2010.

[14] G. García Félix. *Análisis de modelos para la asignación de pérdidas en el cálculo del precio marginal local en el mercado eléctrico mayorista*. PhD thesis, Tecnológico de Monterrey, Monterrey, Mexico, May 2017. In Spanish.

[15] L. Garver. Power generation scheduling by integer programming-development of theory. *Transactions of the American Institute of Electrical Engineers. Part III: Power Apparatus and Systems*, 81(3):730–734, 1962.

[16] A. M. Geoffrion. Primal resource-directive approaches for optimizing non-linear decomposable systems. *Operations Research*, 18(3):375–403, 1970.

[17] E. Gil, J. Bustos, and H. Rudnick. Short-term hydrothermal generation scheduling model using a genetic algorithm. *IEEE Transactions on Power Systems*, 18(4):1256–1264, 2003.

[18] V. Hinojosa-Mateus, L. Pérez-Andrades, and J. Ilić. DC optimal power flow formulation using the power transmission distribution factors – A DIgSILENT programming language application. In F. M. Gonzalez-Longatt and J. L. Rueda, editors, *PowerFactory Applications for Power System Analysis*, volume 139 of *Power Systems*, chapter 5, pages 111–134. Springer, Cham, Switzerland, 2014. ISBN: 978-3-319-12957-0.

[19] B. F. Hobbs, M. H. Rothkopf, R. P. O'Neill, and H. Chao, editors. *The Next Generation of Electric Power Unit Commitment Models*, volume 36 of *International Series in Operations Research and Management Science*. Springer, Boston, USA, 2001.

[20] B. Knueven, J. Ostrowski, and J. P. Watson. A novel matching formulation for startup costs in unit commitment. *Mathematical Programming Computation*, 12(2):225–248, 2020.

[21] D. P. Kotharij and S. Dhillon. *Power System Optimization*. PHI Learning, 2nd edition, 2010.

[22] X. Ma, H. Song, M. Hong, J. Wan, Y. Chen, and E. Zak. The security-constrained commitment and dispatch for Midwest ISO day-ahead co-optimized energy and ancillary service market. In *2009 IEEE Power Energy Society General Meeting*, pages 1–8, Calgary, Canada, July 2009.

[23] C. C. Marín-Cano, J. E. Sierra-Aguilar, J. M. López-Lezama, Á. Jaramillo-Duque, and W. M. Villa-Acevedo. Implementation of user cuts and linear sensitivity factors to improve the computational performance of the security-constrained unit commitment problem. *Energies*, 12 (7):53–72, 2019.

[24] T. V. Menezes and L. C. P. da Suva. A method for transmission loss allocation based on sensitivity theory. In *2006 IEEE Power Engineering Society General Meeting*, pages 1–6, Montreal, Canada, June 2006.

[25] Mexican Secretary of Government. Acuerdo por el que la Secretaría de Energía emite las Bases del Mercado Eléctrico. Diario Oficial de la Federación, 08 September 2015. URL `http://www.dof.gob.mx/nota_detalle.php?codigo=5407715&fecha=08/09/2015`. In Spanish.

[26] Mexican Secretary of Government. Acuerdo por el que se emite el Manual de Costos de Oportunidad. Diario Oficial de la Federación, 16 October 2017. URL `http://dof.gob.mx/nota_detalle.php?codigo=5501341&fecha=16/10/2017`. In Spanish.

[27] Mexican Secretary of Government. Acuerdo por el que se emite el Manual de Mercado de Energía de Corto Plazo. Diario Oficial de la Federación, 17 June 2016. URL `http://dof.gob.mx/nota_detalle.php?codigo=5441705&fecha=17/06/2016`. In Spanish.

[28] G. Morales-España, J. M. Latorre, and A. Ramos. Tight and compact MILP formulation for the thermal unit commitment problem. *IEEE Transactions on Power Systems*, 28(4): 4897–4908, 2013.

[29] G. Morales-España, A. Ramos, and J. García-González. An MIP formulation for joint market-clearing of energy and reserves based on ramp scheduling. *IEEE Transactions on Power Systems*, 29(1):476–488, 2014.

[30] J. Ostrowski, M. F. Anjos, and A. Vannelli. Tight mixed integer linear programming formulations for the unit commitment problem. *IEEE Transactions on Power Systems*, 27(1):39–46, 2012.

[31] D. Sánchez Meléndez. *Metodología de cálculo de las curvas de demanda de reserva para el mercado eléctrico mexicano*. PhD thesis, Tecnológico de Monterrey, Monterrey, Mexico, May 2018. In Spanish.

[32] T. N. Santos, A. L. Diniz, C. H. Saboia, R. N. Cabral, and L. F. Cerqueira. Hourly pricing and day-ahead dispatch setting in Brazil: The DESSEM model. *Electric Power Systems Research*, 189:106709, December 2020.

[33] B. Saravanan, S. Das, S. Sikri, and D. P. Kothari. A solution to the unit commitment problem – a review. *Frontiers in Energy*, 7(2):223–236, 2013.

[34] K. Šepetanc and H. Pandžić. Convex polar second-order Taylor approximation of AC power flows: A unit commitment study. *IEEE Transactions on Power Systems*, 36(4):3585–3594, 2020.

[35] D. A. Tejada-Arango, P. Sánchez-Martın, and A. Ramos. Security constrained unit commitment using line outage distribution factors. *IEEE Transactions on Power Systems*, 33(1): 329–337, 2018.

[36] A. Viana and J. P. Pedroso. A new MILP-based approach for unit commitment in power production planning. *International Journal of Electrical Power & Energy Systems*, 44(1): 997–1005, 2013.

[37] L. Yang, W. Li, Y. Xu, C. Zhang, and S. Chen. Two novel locally ideal three-period unit commitment formulations in power systems. *Applied Energy*, 284:116081, February 2021.

[38] Z. Yu, F. T. Sparrow, B. Bowen, and F. J. Smardo. On convexity issues of short-term hydrothermal scheduling. *International Journal of Electrical Power & Energy Systems*, 22(6): 451–457, 2000.

A Notation

Following this, a summary of sets, indices, parameters, and decision variables are enlisted for quick reference.

Sets and indices of power system:

$\mathcal{BR}$	Set of electric tie-lines; $br \in \mathcal{BR}$
$\mathcal{D}$	Set of elastic loads; those loads are sensitive to price variations; $d \in \mathcal{D}$
$\mathcal{DF}$	Set of fixed loads; $d \in \mathcal{DF}$
$\mathcal{I}$	Set of time period in the planning horizon; $i, i' \in \mathcal{I}$
$\mathcal{N}$	Set for electric nodes in the system; $n \in \mathcal{N}$
$\mathcal{R}$	Set of reserve zones; $r \in \mathcal{R}$
$\mathcal{RO}$	Set of operative ranges of generators with operating prohibited zones; $ro \in \mathcal{RO}$, only for the $\mathcal{U}^{\text{TE}}$ and $\mathcal{U}^{\text{HI}}$ subsets
$\mathcal{U}$	Set of all generators in the system; $u \in \mathcal{U} = \mathcal{U}^{\text{TE}} \cup \mathcal{U}^{\text{HI}} \cup \mathcal{U}^{\text{RE}}$
$\mathcal{U}^{\text{HI}}$	Set of hydroelectric generators; $u \in \mathcal{U}^{\text{HI}}$
$\mathcal{U}^{\text{HI}}$	Set of renewable generators in the system; $u \in \mathcal{U}^{\text{HI}}$
$\mathcal{U}^{\text{TE}}$	Set of thermal generators; $u \in \mathcal{U}^{\text{TE}}$.

Sets and indices of hydraulic system:

$\mathcal{E}$ Set of reservoirs; $e \in \mathcal{E}$

$\mathcal{HI}_e$ Set of hydroelectric generators located in reservoir $e \in \mathcal{E}$; $u \in \mathcal{HI}_e$

$\mathcal{HI}_v$ Set of hydroelectric generators that discharge water over a river $v \in \mathcal{V}_e^{\mathrm{r}}$; $u \in \mathcal{HI}_v$

$\mathcal{V}_e^{\mathrm{c}}$ Set of a rivers converging to reservoir $e \in \mathcal{E}$; $v \in \mathcal{V}_e^{\mathrm{c}}$

$\mathcal{V}_e^{\mathrm{r}}$ Set of a rivers diverging from reservoir $e \in \mathcal{E}$; $v \in \mathcal{V}_e^{\mathrm{r}}$

Sets and indices of economics:

$\mathcal{B}_d^{\mathrm{e.p.b.}}$ Set of segments of the energy purchase bid curve for a elastic load $d \in \mathcal{D}$; $b \in \mathcal{B}_d^{\mathrm{e.p.b.}}$

$\mathcal{B}_u^{\mathrm{e.s.o.}}$ Set of segments of the energy sale offer curve for a generator $u \in \mathcal{U}$; $b \in \mathcal{B}_u^{\mathrm{e.s.o.}}$

$\mathcal{B}^{\mathrm{r.r.}}$ Set of segments of regulation reserve curve; $b \in \mathcal{B}^{\mathrm{r.r.}}$

$\mathcal{B}^{\mathrm{10.s.r.}}$ Set of segments of 10 minutes spinning reserve curve; $b \in \mathcal{B}_u^{\mathrm{10.s.r.}}$

$\mathcal{B}^{\mathrm{10.r.}}$ Set of segments of 10 minutes reserve curve; $b \in \mathcal{B}^{\mathrm{10.r.}}$

$\mathcal{B}^{\mathrm{30.r.}}$ Set of segments of 30 minutes reserve curve; $b \in \mathcal{B}^{\mathrm{30.r.}}$

$\mathcal{B}^{\mathrm{o.r.d.c}}$ Set of segments of operative reserve demand curve; this set represents the requirements of reserve of the ISO and is formed by the subsets of segments of required regulation $\mathcal{B}^{\mathrm{r.r}}$, the spinning reserve of 10 minutes $\mathcal{B}^{\mathrm{10.s.r}}$, the reserve of 10 minutes $\mathcal{B}^{\mathrm{10.r}}$, and the reserve of 30 minutes $\mathcal{B}^{\mathrm{30.r}}$. Thus, $\mathcal{B}^{\mathrm{o.r.d.c}}$ are comprised by $\mathcal{B}^{\mathrm{r.r.}} \bigcup \mathcal{B}^{\mathrm{10.s.r.}} \bigcup \mathcal{B}^{\mathrm{10.r.}} \bigcup \mathcal{B}^{\mathrm{30.r.}}$; $b \in \mathcal{B}^{\mathrm{o.r.d.c}}$

$\mathcal{S}_u$ Set of start-up cost curve segments for a thermal generator u; $s \in \mathcal{S}_u$; $u \in \mathcal{U}^{\mathrm{TE}}$. The start-up cost depends on how long a generator has been offline

Parameters:

$AR_{u,s}$ Start-up offer in a thermal generator $u \in \mathcal{U}^{\mathrm{TE}}$ with a set of segment time $s \in \mathcal{S}_u$; it determines the starting cost by locating a cost in a segment time s in the intervals $[\underline{T}_{u,s}, \overline{T}_{u,s})$; in \$/h

$a_{1,u}, a_{2,u}, a_{3,u}$ Coefficients that are part of the constant term of the HPF (40) for a generator $u \in \mathcal{U}^{\mathrm{HI}}$; in MW

$b_{1,u}, b_{2,u}, b_{3,u}$ Linear coefficients that are part of the constant term of the HPF (40) for a generator $u \in \mathcal{U}^{\mathrm{HI}}$; in MW/m

$c_{1,u}, c_{2,u}, c_{3,u}$ Quadratic coefficient that is part of the constant term of the HPF (40) for a generator $u \in \mathcal{U}^{\mathrm{HI}}$; in MW s/m^2

$DB_{b,d,i}$ Price-sensitive demand bid in a segment $b \in \mathcal{B}_u^{\mathrm{e.p.b.}}$ for a load $d \in \mathcal{D}$ in a period $i \in \mathcal{I}$; in \$/MW

$DF_{d,i}$ Fixed demand in a segment $d \in \mathcal{DF}$ in a period $i \in \mathcal{I}$; in MW

$\overline{fn}_{br,i}, \overline{fp}_{br,i}$ Maximum value for the power counterflow and flow on tie-line $br \in \mathcal{BR}$ in a period $i \in \mathcal{I}$, respectively; in MW. These parameters refer to the amount of energy that a tie-line can transmit safely in one direction or reverse

$\overline{g}_{u,i}, \underline{g}_{u,i}$ Maximum and minimum generation value of a generator $u \in \mathcal{U}$ in a period $i \in \mathcal{I}$, respectively; in MW

$\overline{g}^{RE}_{u,ro,i}, \underline{g}^{RE}_{u,ro,i}$	Maximum and minimum regulation limit for a operative zone $ro \in \mathcal{RO}$ of a generator $u \in \mathcal{U}^{\mathrm{TE}} \cup \mathcal{U}^{\mathrm{HI}}$ in a period $i \in \mathcal{I}$, respectively; in MW
$\overline{g}^{RO}_{u,ro}, \underline{g}^{RO}_{u,ro}$	Maximum and minimum operation limit for a operative zone $ro \in \mathcal{RO}$ of a generator $u \in \mathcal{U}$ respectively; in MW
g^{sync}_u	Power generation of a generator $u \in \mathcal{U}$ injects into the system immediately after connecting it; in MW
$GB_{b,u,i}$	Offer quantity of $b \in \mathcal{B}^{\mathrm{e.p.b.}}_u$ for $u \in \mathcal{U}^{\mathrm{TE}} \cup \mathcal{U}^{\mathrm{RE}}$ in a period $i \in \mathcal{I}$; in MW
$LSF_{n,i}$	Sensitivity transmission losses in node $n \in \mathcal{N}$ with regard to changes in power injections in node $n \in \mathcal{N}$ in a period $i \in \mathcal{I}$; dimensionless
$Mrre_{u,i}$	Minimum regulation reserve that can be committed to a generator $u \in \mathcal{U}^{\mathrm{TE}} \cup \mathcal{U}^{\mathrm{HI}}$ in a period $i \in \mathcal{I}$; in MW
mgc_u	Minimum operating cost of a thermal generator $u \in \mathcal{U}^{\mathrm{TE}}$ that works at least at minimum power $\underline{g}_u$; in \$
$\overline{NP}_u$	Maximum number of stoppages allowed for a generator $u \in \mathcal{U}^{\mathrm{TE}} \cup \mathcal{U}^{\mathrm{HI}}$ during the planning horizon; dimensionless
N_i	Minimum number of generators to be committed for regulation reserve in $i \in \mathcal{I}$; dimensionless
$ORDC_{b,i}$	Operating reserve demand curve bid on $b \in \mathcal{B}^{\mathrm{o.r.d.c}}$ in a period $i \in \mathcal{I}$; in MW
$P^{\mathrm{e.p.b.}}_{b,d,i}$	Price of energy purchase offer in a segment $b \in \mathcal{B}^{\mathrm{e.p.b.}}_u$ for load $d \in \mathcal{D}$ in a period $i \in \mathcal{I}$; in \$/MWh
$P^{\mathrm{e.s.o.}}_{b,u,i}$	Price of energy sale offer in a segment $b \in \mathcal{B}^{\mathrm{e.s.o.}}_d$ for a generator $u \in \mathcal{U}^{\mathrm{TE}} \cup \mathcal{U}^{\mathrm{HI}}$ in a period $i \in \mathcal{I}$; in \$/MWh
$P^{\mathrm{o.c}}_{u,i}$	Opportunity cost of an hydroelectric generator $u \in \mathcal{U}^{\mathrm{HI}}$ in a period $i \in \mathcal{I}$; in \$/MWh. This data comes from the monthly and weekly planning processes that consider the future cost of water
$P^{\mathrm{10.s.r.o}}_{u,i}$	Price of 10 minutes spinning reserve offer of a generator $u \in \mathcal{U}$ in a period $i \in \mathcal{I}$; in \$/MWh
$P^{\mathrm{10.n.s.r.o}}_{u,i}$	Price of 10 minutes non-spinning reserve offer of a generator $u \in \mathcal{U}$ in a period $i \in \mathcal{I}$; in \$/MWh
$P^{\mathrm{30.s.r.o}}_{u,i}$	Price of 30 minutes spinning reserve offer of a generator $u \in \mathcal{U}$ in a period $i \in \mathcal{I}$; in \$/MWh
$P^{\mathrm{30.n.s.r.o}}_{u,i}$	Price of 30 minutes non-spinning reserve offer of a generator $u \in \mathcal{U}$ in a period $i \in \mathcal{I}$; in \$/MWh
$P^{\mathrm{r.r.o}}_{u,i}$	Price of regulation reserve offer of a generator $u \in \mathcal{U}$ in a period $i \in \mathcal{I}$; in \$/MWh
$P^{\mathrm{o.r.d.c}}_{b,i}$	Price of operative reserve demand curve on $b \in \mathcal{B}^{\mathrm{o.r.d.c}}$ in a period $i \in \mathcal{I}$; in \$/MWh
$PTDF_{br,n,i}$	Power transmission distribution factors are the incremental changes or sensitivity power flow in tie-lines $br \in \mathcal{BR}$ with respect to power injection at any node $n \in \mathcal{N}$ in a period i

q_u^{mxef}	Water discharge at maximum efficiency of a generator $u \in \mathcal{U}^{\mathrm{HI}}$; in m^3/s
$\overline{q}_{u,i}, \underline{q}_{u,i}$	Maximum and minimum water flow passing through the turbines of a generator $u \in \mathcal{U}^{\mathrm{HI}}$ in a period $i \in \mathcal{I}$, respectively; in m^3/s
$\overline{Q}_{v,i}, \underline{Q}_{v,i}$	Maximum and minimum water discharge limits over a river $v \in \mathcal{V}_e^{\mathrm{r}}$ in a reservoir $e \in \mathcal{E}$ in a period $i \in \mathcal{I}$, respectively; in m^3/s
R_{br}	Electric resistance of a tie-line $br \in \mathcal{BR}$; dimensionless
RB_u	Ramp-down rate is the capacity of a generator $u \in \mathcal{U}^{\mathrm{TE}} \cup \mathcal{U}^{\mathrm{HI}}$ to decrease power between two consecutive periods; in MW/h
$RE_{u,i}^{10}$	Emergency ramp rate for 10 minutes spinning reserve of a generator $u \in \mathcal{U}$ in a period $i \in \mathcal{I}$; in MW
$RE_{u,i}^{30}$	Emergency ramp rate for 30 minutes reserve of a generator $u \in \mathcal{U}$ in a period $i \in \mathcal{I}$; in MW
$RR_{u,i}$	Regulation ramp rate of a generator $u \in \mathcal{U}$ in a period $i \in \mathcal{I}$; in MW
RS_u	Ramp-up rate rate is the capacity of a generator $u \in \mathcal{U}^{\mathrm{TE}} \cup \mathcal{U}^{\mathrm{HI}}$ to increase; power between two consecutive periods; in MW/h
RS_u^{sync}	Ramp-up rate of a generator is the capacity of a generator $u \in \mathcal{U}^{\mathrm{TE}}$ to increase power when the generator is starting; in MW/h
$RRo_{u,i}^{10}$	10 minutes spinning reserve bid of a generator $u \in \mathcal{U}^{\mathrm{TE}} \cup \mathcal{U}^{\mathrm{HI}}$ in a period $i \in \mathcal{I}$; in MW
$RRo_{u,i}^{30}$	30 minutes spinning reserve bid of a generator $u \in \mathcal{U}^{\mathrm{TE}} \cup \mathcal{U}^{\mathrm{HI}}$ in a period $i \in \mathcal{I}$; in MW
$RNR_{u,i}^{10}$	10 minutes non-spinning reserve bid of a offline generator $u \in \mathcal{U}^{\mathrm{TE}} \cup \mathcal{U}^{\mathrm{HI}}$ in a period $i \in \mathcal{I}$; in MW
$RNR_{u,i}^{30}$	30 minutes non-spinning reserve bid of a offline generator $u \in \mathcal{U}^{\mathrm{TE}} \cup \mathcal{U}^{\mathrm{HI}}$ in a period $i \in \mathcal{I}$; in MW
$RRe_{u,i}$	Regulation reserve bid of a generator $u \in \mathcal{U}^{\mathrm{TE}} \cup \mathcal{U}^{\mathrm{HI}}$ in a period $i \in \mathcal{I}$; in MW
$\overline{RNR}_{u,i}^{10}$	Maximum capacity limit for 10 minutes non-spinning reserve of a generator $u \in \mathcal{U}^{\mathrm{TE}} \cup \mathcal{U}^{\mathrm{HI}}$ in a period $i \in \mathcal{I}$; in MW
$\overline{RNR}_{u,i}^{30}$	Maximum capacity limit for 30 minutes non-spinning reserve of a generator $u \in \mathcal{U}^{\mathrm{TE}} \cup \mathcal{U}^{\mathrm{HI}}$ in a period $i \in \mathcal{I}$; in MW
$\overline{RRo}_{u,i}^{10}$	Maximum capacity limit for 10 minutes spinning reserve of a generator $u \in \mathcal{U}^{\mathrm{TE}} \cup \mathcal{U}^{\mathrm{HI}}$ in a period $i \in \mathcal{I}$; in MW
$\overline{RRo}_{u,i}^{30}$	Maximum capacity limit for 30 minutes spinning reserve of a generator $u \in \mathcal{U}^{\mathrm{TE}} \cup \mathcal{U}^{\mathrm{HI}}$ in a period $i \in \mathcal{I}$; in MW
$\overline{RRe}_{u,ro,i}$	Maximum capacity limit for regulation reserve of a generator $u \in \mathcal{U}^{\mathrm{TE}} \cup \mathcal{U}^{\mathrm{HI}}$ in a operative zone ro in a period $i \in \mathcal{I}$; in MW
$\overline{T}_{u,s}, \underline{T}_{u,s}$	Start and end of start-up cost segment $s \in \mathcal{S}$, respectively; in h

$\bar{t}_u$ are the minimum up-times periods that a generator $u \in \mathcal{U}^{\mathrm{TE}} \cup \mathcal{U}^{\mathrm{HI}}$ must be kept on before turning them off; in h

$\underline{t}_u$ are the minimum down-times periods that a generator $u \in \mathcal{U}^{\mathrm{TE}} \cup \mathcal{U}^{\mathrm{HI}}$ must be kept off before turning them on; in h

ts_u Start-up time for a generator $u \in \mathcal{U}^{\mathrm{TE}}$; in h

$\overline{w}_e, \underline{w}_e$ Maximum and minimum water storage limits on a reservoir $e \in \mathcal{E}$; in m^3

$w_e^{C.I.}$ Water volume in initial conditions on a reservoir $e \in \mathcal{E}$; in m^3

δ_v Water travel time delay of a river $v \in \mathcal{V}_e^{\mathrm{c}}$; in h

$\epsilon_{e,i}$ The amount of water collected through natural inflows in a reservoir $e \in \mathcal{E}$ in a period $i \in \mathcal{I}$; in m^3

$\rho_{e,i}$ Water outflow of a reservoir $e \in \mathcal{E}$ in a period $i \in \mathcal{I}$ used for different purposes unrelated to energy generation like irrigation or human consumption; in m^3

$\kappa_{v,i}$ Discharge spillage over a river $v \in \mathcal{V}_e^{\mathrm{r}}$ in a period $i \in \mathcal{I}$; in m^3. It is the amounts to the water released through the river without passing through the turbines

Binary variables:

$sa_{u,i,s}$ Equal to 1 if generator $u \in \mathcal{U}^{\mathrm{TE}}$ have a start up type $s \in \mathcal{S}$ in period $i \in \mathcal{I}$, and 0 otherwise

$\alpha_{u,i}$ Equal to 1 if generator $u \in \mathcal{U}^{\mathrm{TE}} \cup \mathcal{U}^{\mathrm{HI}}$ starts up at the beginning of period $i \in \mathcal{I}$, and 0 otherwise

$\tau_{u,i}$ Equal to 1 if generator $u \in \mathcal{U}^{\mathrm{TE}} \cup \mathcal{U}^{\mathrm{HI}}$ is shut-down at the beginning of period $i \in \mathcal{I}$, and 0 otherwise

$\beta_{u,i}$ Equal to 1 if generator $u \in \mathcal{U}^{\mathrm{TE}} \cup \mathcal{U}^{\mathrm{HI}}$ is online in a period $i \in \mathcal{I}$, and 0 otherwise

$\beta_{u,i}^{s}$ Equal to 1 if generator $u \in \mathcal{U}^{\mathrm{TE}}$ is starting-up in a period $i \in \mathcal{I}$, and 0 otherwise

$\beta_{u,ro,i}^{RO}$ Equal to 1 if generator $u \in \mathcal{U}^{\mathrm{TE}} \cup \mathcal{U}^{\mathrm{HI}}$ is in operating range $ro \in \mathcal{RO}$ in a period $i \in \mathcal{I}$, and 0 otherwise

$\beta_{u,ro,i}^{RE}$ Equal to 1 if generator $u \in \mathcal{U}^{\mathrm{TE}} \cup \mathcal{U}^{\mathrm{HI}}$ is in regulation reserve re in a period $i \in \mathcal{I}$, and 0 otherwise

$\beta_{u,i}^{rnr10}$ Equal to 1 if generator $u \in \mathcal{U}^{\mathrm{TE}} \cup \mathcal{U}^{\mathrm{HI}}$ is in 10 minutes non-spinning reserve $rnr10$ in a period $i \in \mathcal{I}$, and 0 otherwise

$\beta_{u,i}^{rnr30}$ Equal to 1 if generator $u \in \mathcal{U}^{\mathrm{TE}} \cup \mathcal{U}^{\mathrm{HI}}$ is in 30 minutes non-spinning reserve $rnr30$ in a period $i \in \mathcal{I}$, and 0 otherwise

Real variables:

$db_{b,d,i}$ Amount of demand price-response of segment b for demand $d \in \mathcal{D}$ in a period $i \in \mathcal{I}$, in MW

$g_{u,i}$ Amount of power a generator $u \in \mathcal{U}^{\mathrm{TE}} \cup \mathcal{U}^{\mathrm{HI}}$ produces in a period $i \in \mathcal{I}$, in MW

$gb_{b,u,i}$ Amount of power a generator $u \in \mathcal{U}^{\mathrm{TE}} \cup \mathcal{U}^{\mathrm{HI}}$ produces in segment b of period $i \in \mathcal{I}$, in MW

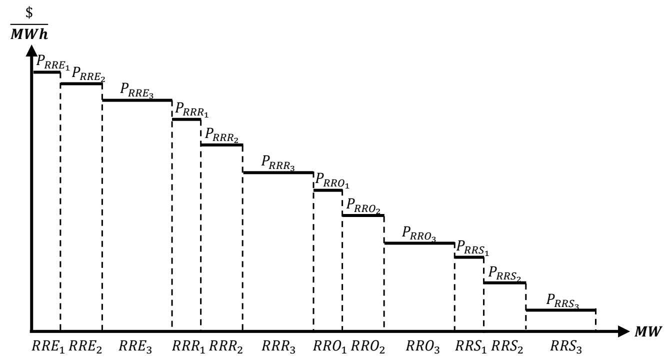

Figure 13: Operative reserve demand curve.

$gs_{u,i}$	Amount of power a generator u produces during the start-up time in a period $i \in \mathcal{I}$, in MW
$h_{v,i}$	Net hydraulic head of a river v in a period $i \in \mathcal{I}$; in m
$iny_{n,i}$	Amount of power input at node $n \in \mathcal{N}$ in a period $i \in \mathcal{I}$, in MW
$Loss_i^{SP}$	Amount of exact transmission losses in a period $i \in \mathcal{I}$, in MW
$Loss_i^{MP}$	Amount of approximate transmission losses in a period $i \in \mathcal{I}$, in MW
$rro_{u,i}^{10}$	Amount of 10 minutes spinning reserve of generator u in a period $i \in \mathcal{I}$, in MW
$rnr_{u,i}^{10}$	Amount of 10 minutes non-spinning reserve of generator u in a period $i \in \mathcal{I}$, in MW
$rro_{u,i}^{30}$	Amount of 30 minutes spinning reserve of generator u in a period $i \in \mathcal{I}$, in MW
$rnr_{u,i}^{30}$	Amount of 30 minutes non-spinning reserve of generator u in a period $i \in \mathcal{I}$, in MW
$rre_{u,i}$	Amount of regulation reserve of generator u in a period $i \in \mathcal{I}$; in MW
$rco_{b,i}$	Amount of reserve (regulation, 10 minutes spinning and non-spinning reserve, 30 minutes spinning, and non-spinning reserve) commitment of the operative reserve demand curve on segment b in a period $i \in \mathcal{I}$; in MW
$q_{u,i}$	Water discharge of generator u in a period $i \in \mathcal{I}$; in m^3/s
$w_{e,i}$	Water volume in the reservoir e in a period $i \in \mathcal{I}$; in m^3

B Reserve requirements

The reserve requirements that established by the ISO that are to be met by generators. The type of reserve requirements are regulation $RRE_{b,i}$, spinning $RRR_{b,i}$, operative $RRO_{b,i}$, and supplementary $RRS_{b,i}$ for each step $b \in \mathcal{B}_d^{\text{o.r.d.c}}$ for each period i. To introduce the reserve requirements the ISO uses an ORDC that is a staircase function with decreasing features. In Mexico, ORDC has twelve steps b that are comprised by the price of the reserves $P_{b,i}^{o.r.d.c}$ and the amount of reserve $ORDC_{b,i}$ for each requirement $RRE_{b,i}$, $RRR_{b,i}$, $RRO_{b,i}$ and $RRS_{b,i}$ (three steps for each requirement) in terms of MWh. A representation of a ORDC is displayed in Figure 13.

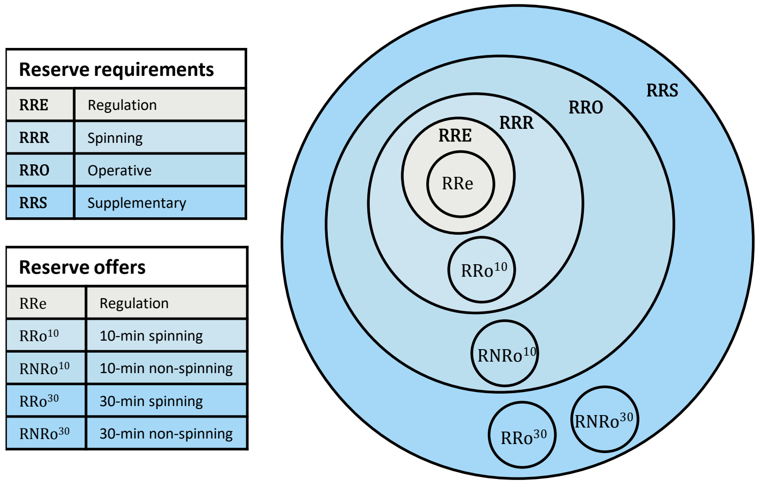

Figure 14: Relationship between requirements and reserves offers.

Figure 14 illustrates the relationship between the requirements and the reserves. The circles represent both the reserve offers ($RRe_{u,i}$,$RRo^{10}_{u,i}$,$RNRo^{10}_{u,i}$,$RRo^{30}_{u,i}$,$RNRo^{30}_{u,i}$) and the reserve requirements. On the one hand, to meet the reserve-requirements the generators must make enough reserve-offers. When a reserve-offers circle is within a reserve-requirement circle this reserve-offer contributes to meet this requirement. For instance, $RRe_{u,i}$ (offer) contributes to meet the $RRE_{b,i}$ (requirement) while it also contributes to meet simultaneously the requirements $RRR_{b,i}$, $RRO_{b,i}$ and $RRS_{b,i}$. It is worth noting that offers corresponding to RRo^{30} and $RNRo^{30}$ contribute only to meet the $RRS_{b,i}$ but do not contribute to meet the regulation requirement $RRE_{b,i}$. On the other hand, when a requirement is located within another this means that it will be partially met other requirements within it. For instance, $RRR_{b,i}$ is partially met when $RRE_{b,i}$ is met. Similarly, $RRO_{b,i}$ is partially met when the $RRE_{b,i}$ and $RRR_{b,i}$ are met. Finally, $RRS_{b,i}$ is met when the $RRE_{b,i}$, $RRR_{b,i}$, and $RRO_{b,i}$ are met and the offers $RRo^{30}_{u,i}$ and $RNRo^{30}_{u,i}$ are enough.

C Linearization of the hydro power function

The method begins by transforming the constraint (40) in a function that depends on the flow $q_{u,i}$ and the volume $w_{e,i}$.

$$\begin{aligned} g_{u,i} =& \beta_{u,i}\big((A_{1,u} + B_{1,u}w_{v,i} + C_{1,u}w^2_{v,i}) + (A_{2,u} + B_{2,u}w_{v,i} + C_{2,u}w^2_{v,i})q_{u,i} \\ &+ (A_{3,u} + B_{3,u}w_{v,i} + C_{3,u}w^2_{v,i})q^2_{u,i}\big), \qquad u \in \mathcal{HI}_v,\ v \in \mathcal{V}^{\mathrm{r}}_e,\ e \in \mathcal{E},\ i \in \mathcal{I} \end{aligned} \tag{58}$$

Then, parameters $\{A_{1,u}, ..., C_{3,u}\}$ of Equation (58) can be calculated from parameters $\{a_{1,u}, ..., c_{3,u}\}$ of constraint (40). An equivalent approximation between both constraints is shown in the following sets of equations:

$$
\begin{aligned}
A_{q,u} &= a_{q,u}, && u \in \mathcal{HI}_v,\ q = 1,2,3 && (59)\\
B_{q,u} &\approx \frac{b_{q,u} h^*_{v,i}}{w^*_{e,i}}, && u \in \mathcal{HI}_v,\ u \in \mathcal{V}^{\mathrm{r}}_e,\ e \in \mathcal{E},\ i \in \mathcal{I},\ q = 1,2,3 && (60)\\
C_{q,u} &\approx \frac{c_{q,u} (h^*_{v,i})^2}{(w^*_{e,i})^2}, && u \in \mathcal{HI}_v,\ u \in \mathcal{V}^{\mathrm{r}}_e,\ e \in \mathcal{E},\ i \in \mathcal{I},\ q = 1,2,3 && (61)
\end{aligned}
$$

Parameters $w^*_{e,i}$ are the water volume obtained by the MP in each iteration. The non-linear function (41) is used to obtain the effective head height $h^*_{v,i}$.

Subsequently, equation (58) is linearized using the first-order Taylor polynomial method for two variables ($w_{e,i}$ and $q_{u,i}$) around the volume in current conditions ($w^*_{e,i}$ and $q^*_{u,i}$).

The first time the MP is solved, the $w^*_{e,i}$ is the initial volume $w_{e,0}$. Moreover, $q^*_{v,i}$ is the value of the flow in the turbine, at maximum efficiency according to its design features.

$$
g_{u,i} \leq \beta_{u,i} QW_{u,e,i} + Q_{u,e,i} q_{u,i} + W_{u,e,i} w_{e,i}, \qquad u \in \mathcal{HI}_e,\ e \in \mathcal{E},\ i \in \mathcal{I} \tag{62}
$$

where $QW_{u,e,i}$, $Q_{u,e,i}$ and $W_{u,e,i}$ are found with: Equations (63), (64), and (65), respectively:

$$
\begin{aligned}
QW_{u,e,i} &= \big(g_{u,i}(q_{u,i}, w_{e,i}) - Q_{u,e,i} q_{u,i} - W_{u,e,i} w_{e,i}\big) && u \in \mathcal{HI}_e,\ e \in \mathcal{E},\ i \in \mathcal{I} && (63)\\
Q_{u,e,i} &= A_{2,u} + B_{2,u} w_{e,i} + C_{2,u} (w_{e,i})^2 && &&\\
&\quad + 2(A_{3,u} + B_{3,u} w_{e,i} + C_{3,u} (w_{e,i})^2\big) q_{u,i}, && u \in \mathcal{HI}_e,\ e \in \mathcal{E} && (64)\\
W_{u,e,i} &= B_{1,u} + B_{2,u} q_{u,i} + B_{3,u} (q_{u,i})^2 && &&\\
&\quad + 2(C_{1,u} + C_{2,u} q_{u,i} + C_{3,u} ((q_{u,i})^2) w_{e,i}, && u \in \mathcal{HI}_e,\ e \in \mathcal{E} && (65)
\end{aligned}
$$

Finallly, the water levels $w^*_{e,i}$ and $h^*_{v,i}$ are updated in each iteration k of Algorithm 1. Furthermore, The streamlining of parameters from Equation (59) to Equation (61) is carried out in each iteration too. It is worth mentioning that the accuracy of the Taylor approximation depends on the number of iterations of the algorithm.